AD-A087 622 HARVARD UNIV CAMBRIDGE MA GORDON MCKAY LAB F/G 20/8
QUASICONTINUUM PHYSICS.(U)
JUL 80 E YABLONOVITCH, N BLOEMBERGEN N00014-78-C-0531
UNCLASSIFIED NL

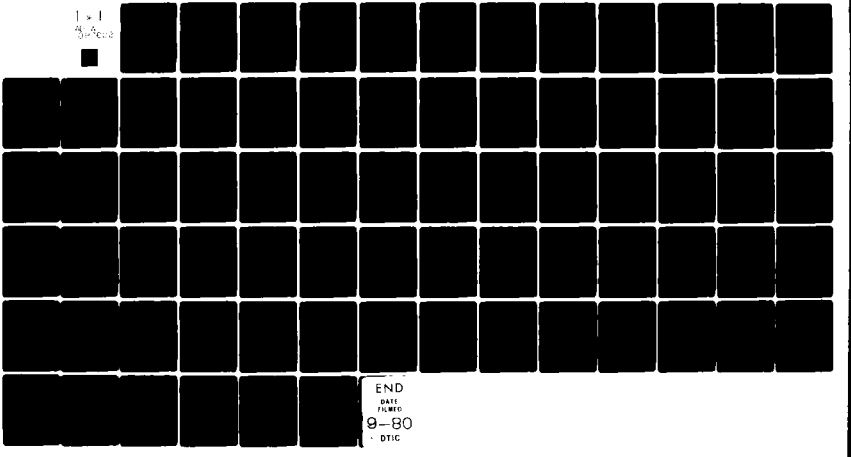

END
DATE FILMED
9-80
DTIC

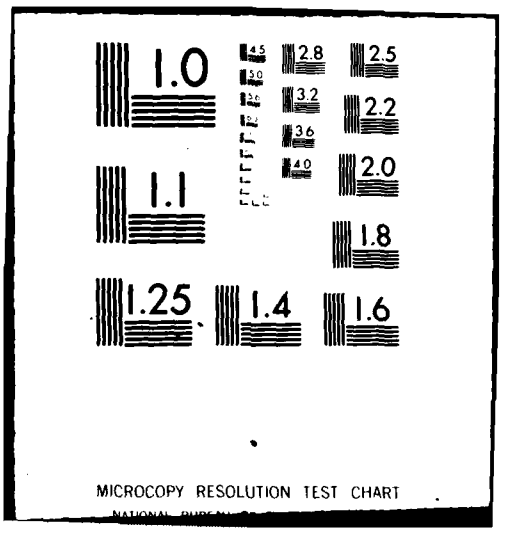
1.0
1.1
1.25
1.4
1.6
1.8
2.0
2.2
2.5
2.8
3.2
3.6
4.0
4.5
5.0
MICROCOPY RESOLUTION TEST CHART

LEVEL II

AD A087622

Gordon McKay Laboratory
Division of Applied Sciences
Harvard University
Cambridge, Massachusetts 02138

FINAL TECHNICAL REPORT
covering the period July 1, 1978 - June 30, 1980

for

ONR Contract N00014-78-C-0531

"Quasicontinuum Physics"

Principal Investigator: Prof. Eli Yablonovitch

July 1980

DISCLAIMER NOTICE

THIS DOCUMENT IS BEST QUALITY PRACTICABLE. THE COPY FURNISHED TO DTIC CONTAINED A SIGNIFICANT NUMBER OF PAGES WHICH DO NOT REPRODUCE LEGIBLY.

Unclassified

SECURITY CLASSIFICATION OF THIS PAGE (When Data Entered)

REPORT DOCUMENTATION PAGE	READ INSTRUCTIONS BEFORE COMPLETING FORM
1. REPORT NUMBER: Final Technical Report	2. GOVT ACCESSION NO.: AD-A087622
3. RECIPIENT'S CATALOG NUMBER	
4. TITLE (and Subtitle): QUASI-CONTINUUM PHYSICS.	5. TYPE OF REPORT & PERIOD COVERED: Final Technical Report, ~~3/1/78-6/30/80~~ 1 Jul 78-30 Jun 80
6. PERFORMING ORG. REPORT NUMBER	
7. AUTHOR(s): Eli Yablonovitch Principal Investigator N. Bloembergen	8. CONTRACT OR GRANT NUMBER(s): N00014-78-C-0531
9. PERFORMING ORGANIZATION NAME AND ADDRESS: Division of Applied Sciences Harvard University Cambridge, MA 02138	10. PROGRAM ELEMENT, PROJECT, TASK AREA & WORK UNIT NUMBERS
11. CONTROLLING OFFICE NAME AND ADDRESS: Office of Naval Research Physics Program Office (Code 421) 800 N. Quincy Street, Arlington, VA 22217	12. REPORT DATE: Jul 80 13. NUMBER OF PAGES
14. MONITORING AGENCY NAME & ADDRESS (if different from Controlling Office): 12 72	15. SECURITY CLASS. (of this report): Unclassified 15a. DECLASSIFICATION DOWNGRADING SCHEDULE

16. DISTRIBUTION STATEMENT (of this Report)

Approved for public release; distribution unlimited.

17. DISTRIBUTION STATEMENT (of the abstract entered in Block 20, if different from Report)

18. SUPPLEMENTARY NOTES

19. KEY WORDS (Continue on reverse side if necessary and identify by block number)

Infrared-infrared double resonance, subnanosecond CO_2 laser pulses, polyatomic molecules, visible-infrared double resonance, fluorescence, vibrational excitation.

20. ABSTRACT (Continue on reverse side if necessary and identify by block number)

Polyatomic molecules are prepared in highly excited vibrational states by short high intensity CO_2 laser pulses. The excited state is probed by a second infrared pulse, or by visible fluorescence. An apparatus involving two independently tunable infrared pulses permits time-resolved infrared spectroscopy intramolecular interactions. Visible-infrared double pulse experiments permit the study of quasi-continuum vibrational absorption in an electronically excited state of the molecule.

DD FORM 1 JAN 73 1473 EDITION OF 1 NOV 65 IS OBSOLETE
S/N 0102-014-6601

Unclassified
SECURITY CLASSIFICATION OF THIS PAGE (When Data Entered)

157000

1. Introduction

The techniques of sub-nanosecond CO_2 laser pulse generation have been used to probe the properties of molecules with very high vibrational energy. In polyatomic molecules the density of vibrational states becomes so high that one may speak of a quasi-continuum of vibrational energy levels. The properties of such molecules are of great current interest in connection with the problems of laser induced isotope separation and laser induced (mode-selective) chemistry. Questions of intramolecular energy transfer and relaxation have been studied under this contract by two distinct categories of experiments. These are briefly described in the following two sections. More detailed results may be found in the three papers, published or submitted for publication, which are attached as appendices.

2. Infrared-Infrared Double Picosecond Irradiation

In these experiments a first pulse of CO_2 laser radiation with a pulse duration which may be varied from 2×10^{-7} sec to 3×10^{-11} sec is used to give the molecule a high vibrational excitation. The absorption has been measured as a function of pulse duration and intensity. Results are presented in Appendix 1. A second infrared pulse, with a variable delay, is then used to probe the infrared absorption spectrum. In the original experiment the two pulses were at the same frequency and were obtained by means of a beam splitter.

During this contract apparatus has been constructed in which the outputs of two independently tunable CO_2 lasers are switched by the same plasma switch. The first pulse at the P(20) CO_2 line is used to pump the

ν_3 mode of the SF_6 molecule. The change in absorption of the SF_6 molecule is probed by the second tunable pulse. A 30 picosecond resolution has been obtained over a frequency interval 18 cm^{-1} to the low frequency side and 9 cm^{-1} to the high frequency side of the P(20) pump line. Preliminary analysis of the data indicates that the energy redistribution from the ν_3 mode to the other modes takes less than 30 picoseconds. Alternatively, one might say that the intense picosecond pulse immediately excites a superposition of modes in the quasi-continuum. It is planned to continue these experiments with other funding. The experimental facility is unique and well suited to address some outstanding questions in the field of intramolecular relaxation of highly excited states.

3. Infrared-Visible Double Pulse Excitation

These experiments utilize 10-20 nanosecond pulses from a TEA CO_2-laser and from a pulsed dye laser pumped by the fundamental or second harmonic of a ruby laser. In the experiments carried out on NO_2 and biacetyl, the molecule was first pumped to an electronic excited state with the visible pulse. A quasi-continuum absorption of infrared absorption is then possible in the excited manifold. In the electronic ground state no infrared absorption at CO_2 laser wave length took place. The infrared absorption in the excited state causes changes in the fluorescence spectrum from this level. A publication on the NO_2 results attached as Appendix 2 is believed to be the first of its kind in this novel type of spectroscopy. More experimental details are described in the paper on biacetyl, which is scheduled for publication in September 1980 in the Journal of Chemical Physics and is attached as Appendix 3.

It is planned to use this double pulse facility in experiments on other molecules, where infrared absorption may occur in the electronic ground state. The question of inverse electronic relaxation needs to be explored further. Experiments on chromyl chloride are under way with temporary support from other sources.

Appendix 1

A STUDY OF COLLISIONLESS MULTIPHOTON ABSORPTION IN SF_6 USING PICOSECOND CO_2 LASER PULSES

H. S. Kwok*, Eli Yablonovitch+ and N. Bloembergen

Gordon McKay Laboratory
Harvard University
Cambridge, Mass 02138

*Present address: Materials and Molecular Research Division, Lawrence Berkeley Laboratory, Berkeley, Ca 94720.

+Present address: Corporate Research Laboratory, Exxon Research and Engineering, Linden, NJ 07036.

ABSTRACT

The dynamics of collisionless infra-red multiphoton absorption in SF_6 was studied using picosecond CO_2 laser pulses. It was found that at this new regime of light-matter interaction at very high laser intensities, the absorption in the quasicontinuum has a considerable intensity dependence. The deviation from energy fluence scaling law was found to begin at about 400 MW/cm^2. Above this intensity, the multiphoton interaction between the laser and the molecule should be described by the full coherent Schrodinger equation rather than by the usual Master rate equations. A novel method of preheating the SF_6 molecules is also described and the saturation behavior of these preheated molecules is measured with the picosecond pulses.

I. INTRODUCTION

Much understanding of the process of infrared laser induced multiphoton absorption (MPA) and dissociation (MPD) has been gained in the past several years.[1a,b,c] It is generally believed that the initial excitation of the polyatomic molecule over the low lying discrete levels contributes to the frequency selectivity and intensity dependence of the overall multiphoton processes. The fact that sharp resonances can occur in MPD has been demonstrated recently by Dai et al.[2] It is also commonly accepted that once the molecule has been excited to the quasicontinuum (QC) of vibrational states where the multitude of energy levels interact strongly with each other, the absorption of energy by the polyatomic molecule will become a linear absorption process. The laser fluence rather than the laser intensity will determine the total energy absorbed by the molecule.[1a,3a,b] When sufficient energy has been absorbed, unimolecular decomposition of the polyatomic molecule will occur in complete agreement with the RRKM theory predictions.

While the general picture is quite clear, there are many questions remaining for a complete understanding of the process of MPD. For example, more quantitative information about the transition from the discrete levels to the QC is needed. More important, there is still the question of the frequency and intensity dependence of the QC adsorption, such as how the energy redistributes among all the vibrational modes and whether there exists any sharp resonance in the QC.

The dynamics of the dissociations, especially if there are several possible decomposition channels are also in need of further study.[4]

Evidently, the best apparatus to study MPD experimentally is a molecular beam machine where in addition to being collision free, the dynamics of the dissociation process can be explored by obtaining both the angular distribution and the time-of-flight spectra of the various dissociation products.[5a,b,] However, there are many situations where we are only interested in having multiphoton excitation in the molecule without dissociating it. Moreover, it is necessary that MPA be understood more thoroughly before any study of MPD can be complete. As a matter of fact, to acquire a thorough understanding of MPA, one should try to avoid dissociation which contributes complications that render the interpretation of the experimental data very difficult. In this paper we shall describe a study of collisionless MPA in SF_6 in a gas cell using picosecond CO_2 laser pulses up to very high levels of excitation without dissociating the molecules.

There are many advantages of using picosecond laser pulses. First of all, with a pulse duration of 30 psec, there can hardly be any collision during the laser pulse interaction, even at cell pressures as high as 20 torr. Thus the stringent requirement on cell pressure for nanosecond pulse experiments can be relaxed by almost a thousand-fold.

Secondly, the peak intensity of a picosecond pulse is at least three orders of magnitude larger than a nanosecond TEA laser pulse with the same fluence. Therefore, one can expect the relative importance of the initial excitation to diminish and hope to study the

QC more directly. However because of exactly the same reason, care should be taken in generalizing the result of this experiment to the ordinary situations using nanosecond TEA CO_2 pulses.

Thirdly, with picosecond pulses, and their accompanying high intensities, there may be a chance of having the up-pumping rate competing with intramolecular energy transfer within the molecule. Hence there exists a possibility of seeing some previously unobserved effects, such as coherent pumping in the quasicontinuum.

The most important advantage is that one can study the SF_6 molecules near or above its dissociation limit without the complications of dissociation and problematic effects such as absorption by dissociation products, because even at very high levels of excitation there can hardly be any dissociation during the laser pulse. For example,[5c] the RRKM lifetime for SF_6 with 10 excess CO_2 photons of energy above its dissociation limit is 7 nsec, which is much longer than the picosecond pulse duration. Therefore one can measure the true MPA characteristics of the SF_6 molecules at very high levels of excitation. This cannot be accomplished with longer duration pulses where dissociation will inadvertently occur during the laser interaction. Therefore, by using picosecond pulses as an excitation source, we should be able to study a new aspect of MPA and hopefully provide new information on the nature of the QC.

We have performed two experiments on measuring the absorption of multiple CO_2 photons by the SF_6 molecule. In the first experiment, we measured the energy deposition with pulses of 30, 50,

90 and 145 psec duration. This provided us with an idea of the importance of pulse intensity in multiphoton interaction in the quasicontinuum. In another experiment, using a method of collisional laser excitation we preheated the SF_6 molecules to the QC and then measured the saturation characteristics of the absorption cross section of SF_6 as it is further excited. This heating method enables us to study molecules which are already in the QC and therefore the question of interference from the discrete levels can be avoided. Since the saturation of any system is closely related to the relaxation mechanism, such a measurement should provide some clues to the nature of intramolecular damping and relaxation in the molecule.

In Section II, we shall describe briefly the picosecond CO_2 laser system used in this experiment. In Section III, the experimental techniques and procedures are described. The data handling methods to obtain the true average number of CO_2 photon absorbed $\langle n \rangle$ and the absorption cross section σ is also discussed. A novel way of thermally heating a polyatomic molecule by a collisional MPA process will then be presented in Section IV. The results of the picosecond measurements are presented in Section V where their significance will also be discussed. A brief conclusion will then be drawn in the final section.

II. THE LASER SYSTEM

The generation of picosecond CO_2 laser pulses using the process of optical free induction decay has been described previously.[6a,b] Essentially, a group of CO_2 molecules are prepared in their upper $(00^{\circ}1)$ lasing level by passing a normal 100 nanosecond TEA laser pulse through a long CO_2 gas tube at high temperature. The traditional way of obtaining optical free induction decay is by Stark-switching the absorbing system out of resonance with the incident laser.[7] The free induction decay will then occur at a slightly different frequency. In our system, we simply turn off the incident laser pulse suddenly using a plasma shutter.[8] The optical free induction decay pulse that follows will be at the same frequency as the incident TEA laser pulse.

The laser system is shown in Fig. 1. A hybrid grating tuned TEA and a low pressure CO_2 laser[9] was employed to provide a single longitudinal mode laser pulse of 100 nsec duration and 5 MW peak power in the TEM_{00} mode. The hydrid configuration was necessary in order to narrow the bandwidth of the CO_2 laser. Moreover, the smooth pulse profile provides much better stability with the plasma shutter, and produces picosecond pulses with very little amplitude fluctuations.

The plasma shutter was a 1:1 telescope with a pair of f/1 germanium lenses. Premature untriggered gas breakdown was prevented by passing clean nitrogen gas through the focal volume. At the peak of the laser pulse, a d.c. spark was fired which in turn triggered the main gas breakdown stopping completely the transmission of the TEA laser

pulse. Since the d.c. spark was triggered by the laser pulse itself,[8] this plasma shutter could be timed extremely precisely and had practically no fluctuation.[10]

Part of the truncated laser pulse was split off using a coated germanium substrate beam splitter, and sent to the SF_6 gas cell after some mild focussing. The remaining portion was sent through a 3 meter long tube containing typically between 50 and 250 torr of CO_2 gas in double pass. The tube was heated to 400°C in order to populate the lower $(10^{\circ}0, 02^{\circ}0)_I$ lasing level thermally. Also, to prevent saturation of absorption by the CO_2 molecules, the TEA laser pulse was spatially filtered before entering the hot gas tube. The optics were arranged such that upon leaving the CO_2 absorption tube, the laser pulse was collimated and has a Gaussian spot size of 3.3 mm in diameter.

As discussed by Yablonovitch et al.,[11] the optical free induction decay pulse at the output of the hot CO_2 gas tube has the same pulse peak power as the input TEA laser pulse. The pulse duration can be approximated by $T_2/\alpha\ell$, where T_2 is the dephasing time of the excitation in the CO_2 gas, α is the linear absorption coefficient and ℓ is the path length. In our system, α has been measured and the result is shown in Fig. 2. This measurement is in agreement with the results of Gerry et al.[12] when scaled to the same temperatures. From Fig. 2 we can obviously distinguish a low pressure regime of Doppler broadening and a high pressure regime of pressure broadening. Since we always operate above 500 torr in the CO_2 gas tube, $\alpha\ell$ can be regarded as a constant with a value of 12.5 nepers.

The pulse durations of the optical free induction decay pulses have been measured with both an autocorrelation method[6] and a double resonance method.[13] The measurements agreed quite well with the prediction of $T_2/\alpha\ell$ for the pulse durations. In our experiments on SF_6, we used CO_2 gas pressures of 40, 70, 140 and 250 torr, corresponding to pulse widths of 145, 90, 50 and 30 psec respectively.

III. EXPERIMENTAL

In the experiments reported here, we measured the mean energy absorbed by the SF_6 molecule, represented in terms of the average number of CO_2 photons $\langle n \rangle$, and the absorption cross section σ of the excited vibrational state of SF_6. We deduced the values of $\langle n \rangle$ and σ as a function of the laser fluence J by observing the attenuation of the laser pulse through a SF_6 gas cell.[14] Provided the experimental data are analyzed properly as discussed below, this method is quite suitable to the study of MPA, especially at low levels of excitation where the optoacoustic method becomes insensitive.[1b]

Before dwelling on the details of the experimental procedure, let us discuss some of the design criteria for the experiment. Most important of all is the energy fluence requirement. The picosecond CO_2 laser pulses we used typically had a peak power of 2 MW. Therefore to generate a fluence of 1 J/cm^2, the laser has to be focussed quite tightly. In our experiments, we used a 50.8 inch focal length AR coated germanium lens for the picosecond laser pulses. For such tight focussing, the corresponding Fresnel length is rather small. The measured beam waist before focussing was 1.65 mm. Using Gaussian optics, for a 50.8 inch focal length, the area of the focussed beam increases by a factor of two at a distance of 3 mm from the focal point. Therefore, in order to ensure a uniform parallel beam in the SF_6 gas cell, the thickness of the gas cell must be smaller than 4 mm.

Another consideration for a more or less uniform laser beam inside the gas-cell was that the transmission must be close to 100%. However, one required the gas cell to be reasonably optically thick in order that the measurement be accurate and sensitive. As a compromise, we limited the transmission of the laser pulse to fall within 50% and 80%. This then imposed a lower limit on the SF_6 gas cell pressure. On the other hand, the gas pressure should be low enough to ensure collisionless interaction. The smallest collisional deactivation time ever measured[15] for SF_6 was 13 nsec-torr. Therefore, in order to avoid any collisional effect in our experiments, we have to limit the SF_6 pressure to be less than 60 torr for a 200 psec pulse. Thus the gas cell length and pressure have to be chosen such that the transmission falls within the range stated above. In our measurements, we typically used a cell pressure of 20 to 30 torr and cell lengths of 1 mm and 3.7 mm.

The experimental setup is shown in Fig. 3. There are two laser beams going into the gas cell. The picosecond pulse was delayed with respect to the truncated pulse by 32 nsec. The truncated preheating pulse was not in use for the energy deposition measurement with room temperature SF_6 molecules. As shall be explained in the next section, the truncated pulse in Fig. 3 was used to thermally heat up the SF_6 molecules. A 635 mm focal length BaF_2 lens was used to focus the truncated pulse onto the gas cell to ensure that all the gas molecules the picosecond pulse sees are uniformly preheated.

The 99.9% SF_6 gas was purchased from Matheson Gas Company without further purification. A Pennalt-Wallace absolute pressure gauge was used to monitor the gas cell pressure. The change in fluence passing through the gas cell was accomplished by moving the calibrated CaF_2 attenuators in front of or behind the gas cell while keeping the total attenuation constant. This allowed us to perform the entire measurement on the same scale of the amplifier and reduced the requirement on the dynamic range of the detection system. The CaF_2 attenuators were sufficiently flat so that no beam deflection occurred while they were moved. To further minimize sensitivity to misalignment onto the detector, the output beam from the gas cell was refocussed onto the detector with a 1:1 magnification.

A liquid nitrogen cooled Ge:Au detector was used throughout the experiments. It was always checked that the detector was well below saturation to ensure a linear response. The detector output was integrated by capacitive loading and displayed on a Tektronix 7904 oscilloscope. Typically many laser shots were taken and the data were averaged. The blackbody radiation produced by the plasma shutter mentioned in the last section was detectable even after a more than 10 m optical path and spatial filtering. They were eliminated by an OCLI 8 μm long wavelength pass filter. All other stray lights were blocked by a diaphram in front of the detector.

NaCl windows were used in the SF_6 gas cells. To make certain that the gas cell was located at the exact focus of the Germanium lens, which was important in determining the laser energy fluence, it

was mounted on a translation stage. To locate the focus, we simply filled the gas cell with SF_6 and moved it back and forth to find the maximum transmission. This procedure ensures that the cell was located at a place of maximum light intensity.

Since we could not measure the picosecond pulse energy directly using an energy meter, the laser fluence was determined indirectly as follows. First of all, using a normal TEA pulse we calibrated the Ge:Au detector integrated voltage output in terms of the true absolute energy using a well-calibrated Scientech power meter. This was done by emptying the hot CO_2 absorption tube and turning off the plasma shutter so that the detector would gel the entire TEA laser pulse. We then filled the CO_2 gas and turned on the plasma shutter to produce the optical free induction decay pulses. Since the detector integration time is much longer than both the TEA laser pulse and the picosecond pulse durations, the output voltage of the detector should simply be proportional to the pulse energy and independent of the pulse shapes. Therefore, from the detector output, we could infer the picosecond pulse energy. Incidentally, the ratio of the picosecond pulse energy and the TEA pulse energy always came out to be simply the ratio of the pulse durations which was expected if the two pulses had the same peak intensities. Since the spatial profile of the picosecond pulse was very close to a Gaussian, we could infer accurately the focal area by measuring the beam size at the entrance of the 2 inch Ge lens, thus completing our estimation of the pulse fluence.

In all measurements, we always checked for the absence of saturation in the CO_2 gas tube which was required in order that the picosecond pulse should have maximum contrast ratio.[6] This is important because the prepulse duration is three orders of magnitude longer than the picosecond pulse. Every precaution must be taken in order not to have the integrated signal from the prepulse interfere with the real signal. After the preliminary checks and calibrations, the experiment can be performed. The transmission T of the SF_6 gas cell was defined as the ratio of the integrated detector signal with the cell filled and at vacuum. The absorption was calculated by

$$\langle n \rangle = \frac{(1 - T)}{NL} \frac{J}{\hbar\omega} \tag{1}$$

where N, L are the number density of molecules and the gas cell path length respectively, and $\hbar\omega$ is the CO_2 photon energy. J is the energy fluence of the laser pulse in J/cm^2. Since it changes its value along the pathway inside the gas cell, some sort of averaging is necessary to get a correct value of J in (1). One can either use the geometrical mean[3] $\sqrt{T}$ J or the arithmetic average of the fluence at the entrance and the exit of the SF_6 cell. The two means are identical provided the transmission is close to unity. In the experiment, we never let the transmission T fall below 50%.

Corresponding to every value of $\langle n \rangle$, we can define a gross absorption cross section σ_G for the molecule

$$\sigma_G = \langle n \rangle \hbar\omega/J \tag{2}$$

We can also obtain the excited state absorption cross section σ given by

$$\sigma = \frac{d\langle n \rangle}{dJ} \hbar\omega \tag{3}$$

This quantity can be thought of as the small signal absorption cross section of a molecule already prepared in its excited state. It is obvious that σ is more physically meaningful than σ_G in investigating the properties of the QC.

Let us discuss now the data reduction procedure that is necessary in this kind of measurements. The main observation about the experimental data is that they are already averaged spatially in the sense that the laser fluence varies across the laser beam. Fortunately, for lasers with a Gaussian profile, there exists an exact deconvolution procedure[16] whereby the truly fluence dependent transmission T can be obtained from the measured transmission $T_M(J)$ by

$$T(J) = T_M(J) \left[1 + \frac{d\ell n T_M(J)}{d\ell n J} \right] \tag{4}$$

Physically, we can think of $T_M(J)$ as the transmission measured with a pulse with spatial profile $J(r) = J_o e^{-2r^2/w_o^2}$ and T(J) as the transmission measured with a pulse of constant spatial profile, e.g.,

$$J(r) = \begin{cases} J_o & r \leq w_o \\ 0 & r > w_o \end{cases} \tag{5}$$

Obviously, formula (4) need not be used if such a laser pulse exists.

Notice that in (4), the correction term $d\ell nT_M/d\ell nJ$ is always negative for a saturating system. Without saturation, i.e., for linear absorption, this term will be zero. It is generally correct that whenever the data is manipulated in any way, new uncertainties will be introduced which will increase the error bars. Fortunately as we shall see later, the saturation of absorption for the picosecond pulses is very small. Hence the correction needed to our raw data was quite small and did not introduce undesirable additional errors.

Once the truly fluence dependent transmission is obtained, $\langle n \rangle$ and σ_G can be calculated using (1) and (2). In principle, σ can be obtained by (3), applying the differentiation on the data for $\langle n \rangle$. In practice it is easier to obtain σ for σ_G employing the relationship

$$\sigma = \sigma_G\left(1 + \frac{d\ell n\sigma_G}{d\ell nJ}\right) \tag{6}$$

This relationship can be obtained from (2) and (3) as follows. Observe that $\langle n \rangle \hbar\omega = \sigma_G J$. Differentiating both sides with respect to J, we obtain

$$\hbar\omega \frac{d\langle n\rangle}{dJ} = \sigma_G + J \frac{d\sigma_G}{dJ} \tag{7}$$

(6) then follows from (7) and (3) after a little algebraic manipulation.

For a system that does not saturate too rapidly in absorption, such as the SF_6 molecules under the irradiance of picosecond pulses, the correction factor in (6) is small and σ is numerically close to σ_G. Therefore it is much better to obtain the absorption cross section from σ_G rather than from $\langle n\rangle$.

IV. THERMAL EXCITATION OF SF_6 USING TRUNCATED CO_2 LASER PULSES

In this section, we shall describe a novel way of obtaining thermally excited SF_6 molecules using collisional laser excitation. In many experiments on MPA and MPD, it is desirable to use SF_6 molecules which are already in the quasicontinuum whereby the discrete levels can be ignored. A brute force method of getting these excited molecules is by heating the entire gas cell to a few hundred degrees. Here we present an alternative method of heating the SF_6 molecules. It has the merits of simplicity, and can be generalized to other molecules in a straight forward manner.

The vibrational excitation in a given polyatomic molecule generally redistributes first among the rotational levels via collisional V-R energy transfer (rotational hole-filling), and then among the various vibrational levels via collisional V-V transfer. It will then be followed by V-T relaxation where the internal energy will equilibrate with the thermal translational energy of the molecule. In ordinary thermal heating, the translational, vibrational and rotational temperatures are the same. However, in MPA interaction, the translational temperature of the molecule does not play any significant role since it only contributes negligible Doppler broadening anyway. Therefore, the molecule can be considered "thermally" excited if the vibrational-rotational temperature has been established, i.e., after the competion of V-R and V-V energy relaxation but not V-T relaxation. For SF_6, the V-R and V-V relaxation times are 150 ns-torr and 1.2 μsec-torr respectively.[17]

Our scheme of "thermally" heating the SF_6 molecules consists of exciting the molecules using a truncated CO_2 laser pulse and then allowing the excitation to relax among the vibrational-rotational states by collisions.

To determine whether the molecules are sufficiently thermalized, we need a reference standard of thermal heating. Nowak and Lyman (NL) measured the absorption cross section of SF_6 molecules using a weak CW CO_2 laser after thermal shock tube heating.[18] Their results provide an excellent calibration standard to test for thermal heating in our experiment. To see that this is the case, we plot in Fig. 4 the absorption cross section σ at P(20) as measured with a truncated TEA CO_2 pulse, at various cell pressures. Since the truncated pulse is ~30 nsec duration, we expect increasingly better thermalization as we increased the cell pressure. Indeed, as seen from Fig. 4, the measured result approached that of the measurement of NL as the pressure increased from 5 to 50 torr. The discrepancies at low values of $\langle n \rangle$ is probably due to the initial bottlenecking effect which is not negligible even at 50 torr for weak excitation pulses.

To further allow the SF_6 molecules to thermalize before we study them with picosecond pulses, we allowed a 32 nsec time delay between the truncated pulse and the picosecond pulse. Moreover for experiments done with thermally heated SF_6, we always turned the CO_2 laser to the P(28) line. This is because the absorption spectrum of SF_6 exhibits a redshift as it is heated. Therefore, to obtain a larger σ, the laser should be correspondingly tuned to the red.

Moreover, the maximum σ as a function of the truncated heating pulse fluence is experimentally very convenient for adjusting the fluence of the heating pulse.

Figure 5 shows the absorption cross section measured by a weak picosecond probe laser pulse when the truncated pulse fluence was varied. The horizontal axis was obtained from an independent measurement of $\langle n \rangle$ versus J using the P(28) truncated pulse. Two different SF_6 cell pressures were used. It can be seen that with 50 torr of SF_6 in the gas cell, the measured σ agrees with the thermal shock tube measurement exactly, indicating that the internal energy deposited by the truncated pulse is fully vibrationally thermalized by collisions. The 20 torr curve in Fig. 5 follows the same pattern but shows considerably saturation of absorption at low fluences. This is presumably due to insufficient collisional population redistribution. The peak σ in Fig. 5 corresponds to a heating pulse fluence of only 0.054 J/cm^2.

We note here that this technique of collisional thermal excitation in a collisionless experiment is possible only because we are using both nanosecond and picosecond laser pulses. 20 Torr of SF_6 in a gas cell is high pressure enough for vibrational and rotational relaxation for the truncated pulse, but at the same time low pressure enough for collisionless interaction with the picosecond pulses. Presumably this technique can be generalized to nanosecond TEA pulse experiments provided a μsec pulse is available for thermal heating.

From NL, the peak of the absorption at P(28) corresponds to a temperature of 650°K. Thus we have an accurate definition of the temperature of the SF_6 molecules before the picosecond pulses arrive.

V. RESULTS AND DISCUSSION

(a) SF_6 at 300°K

Figure 6 presents the data on the average photon number absorbed ⟨n⟩ by an SF_6 molecule as a function of the laser pulse fluence. We made the measurements at four different optical free induction decay pulse durations of 30, 50, 90 and 145 psec, respectively. The data reduction procedure described in Section III has been carefully applied. The data was very reproducible upon repeating the experiment. The only sources of error came from the uncertainty in knowing the laser fluence exactly, together with a ~5% error in reading the signal voltages. So the relative error between the different curves in Fig. 6 should be quite small (10%) while the absolute error was estimated to be 50%. Since the experimental curves are almost straight lines with unity slope, making an error in J will produce the same error in ⟨n⟩. This means that the data point will simply slide along the experimental curve. Hence, the uncertainty in knowing exactly the laser fluence should not alter the absolute position of the experimental curves in Fig. 6.

The experimental results show that at very high intensity levels the energy deposition curves do not have any tendency to saturate and converge near the dissociation threshold. As mentioned in the Introduction, for the range of fluences used, there should not be any dissociation occuring during the laser pulse because of the finite dissociation lifetime[5a] (although dissociation may occur after the laser pulse is gone, it does not affect our measurement). So we were

indeed measuring the true laser absorption by the SF_6 molecules at very high levels of excitation. This is different from experiments done with longer duration pulses where at large $\langle n \rangle$, there may be competition due to dissociations, and complications from absorption by the dissociation products.

One interesting observation is that even at an excitation level as high an $\langle n \rangle = 20$, where all the molecules should be excited to the quasicontinuum, the differences between the various curves persist. This implies that the absorption in the QC is not straightly fluence dependent. To elucidate on the interpretation of the experimental data, we plotted the 30 psec data together with the 500 psec, 30 nsec and 100 nsec data of Black et al.[3b,19] in Fig. 7. Plotted on the same figure is also the derived data of Nowak and Lyman,[18] (see Appendix I). The last curve is a hypothetical case of MPA in SF_6 where the absorption cross section of the SF_6 molecules follow exactly the thermally measured value. This is a very useful curve for comparing with the data obtained using laser pulses, especially in testing the thermal bath model.

Since we are trying to compare the results of two different measurements, it is perhaps imperative to note the differences in experimental conditions and the error limits. The laser pulses used in the experiments of Black et al. were as well characterized as the present paper: their 100 nsec pulse was smoothed by the same technique as described in this paper, the truncated 30 nsec pulses were obtained by a triggered plasma shutter, and the 500 psec pulses

were produced also by the process of optical free induction decay. Their MPA results were obtained by the optoacoustic method. Reference 3b presented a very thorough discussion on the data reduction and the correct handling of various corrections. The procedure used was by fitting the experimental curve with an analytic function, and then performing the Gaussian beam correction. The biggest correction came from the high fluence portion of their data where the accuracy might be complicated by dissociation. However, we are only interested in fluences below 1 J/cm^2 where there is no dissociation and the measured result had very little spatial correction. Therefore there should not be any serious problem in comparing their results with ours.

The biggest source of error in optoacoustic measurements is the absolute calibration of the optoacoustic signal to the real average energy absorbed the molecules. To do so, an energy transmission measurement has to be performed the same way as described in this paper. Other than this extra step of calibration, all the data handling procedures are the same between the present experiment and that of Black et al.

With these limitations in mind, let us examine the various curves in Fig. 7. At low fluences and small number of CO_2 photons absorbed, the shorter duration pulses have much larger absorption. There is almost a two order of magnitude difference in $\langle n \rangle$ between the 30 psec and the 100 nsec data. This is certainly due to the bottlenecking effect[1a] of the discrete levels. However, if absorption in QC is strictly fluence dependent, all the experimental

curves should merge at high intensities with the thermal curve (e). From Fig. 7 this is definitely not the case. Instead, the differences in $\langle n \rangle$ between the different duration pulses persist up to very high excitation levels of $\langle n \rangle \sim 40$, and show no resemblence to curve (e) at all.

The dependence of the energy absorption on the laser intensity in the QC is more transparent if we plot $\langle n \rangle$ as a function of the peak intensity at a fixed energy fluence. Figure 8 presents such a plot at a fixed fluence of 0.2 J/cm^2. The range of intensities almost vary by four orders of magnitude. For $\langle n \rangle < 4$, the increase in energy deposition is attributable simply to the bottlenecking effect of the discrete levels. As the laser intensity is increased, more and more molecules are coupled to the QC where the stepwise energy absorption takes place.

Total transition into the QC is estimated to occur at intensities of 1000 MW/cm^2 by Schulz[21] (Galbraith et al. estimated 40 MW/cm^2 (Ref. [20a])). In this limit, the energy absorbed by the SF_6 molecule should stay constant at a value given by the thermal absorption measurement if energy fluence scaling holds in the QC. From numerical integration of the data of NL (Appendix I), the limiting number of CO_2 photons absorbed by the SF_6 molecule at 0.2 J/cm^2 should be 11.5. The expected behavior from energy scaling law is qualitatively indicated by the dashed line in Fig. 8.[30] However, the observed data do not appear to reach any asymtotic value at all and continue to increase as the laser intensity is increased. The apparent point of

departure from the thermal absorption behavior occurs at 400 MW/cm^2.[31]

It is interesting to note that the picosecond data points in Fig. 8 can be fitted by a straight line of slope 1/2. Since the Rabi frequency is given by

$$\omega_R = \mu E/\hbar \tag{8}$$

where μ is the transition dipole moment and E is the electric field of the laser, the observed result implies that at a fixed laser fluence,

$$\langle n \rangle \propto \omega_R. \tag{9}$$

The role of the Rabi frequency in the QC has never been emphasized in previous theoretical treatments of MPA and MPD in polyatomic molecules.[20a,b,c] The dependence on intensity seems to set in at about 400 MW/cm^2. For TEA CO_2 laser pulses this intensity dependence in the QC can be ignored because of the much lower intensities used. However, for picosecond pulses, the energy fluence scaling law no longer holds and both the laser intensity and total fluence determine the interaction of the laser with the molecule.

Actually, energy scaling which comes from Fermi's golden rule should not be expected to hold for the picosecond pulses. One condition[22,20c] for the golden rule of transition probability to be valid, which is also required of all other perturbative methods is that the "area" of the pulse[23] should be much smaller than unity.

The area of the pulse can be approximated by $\omega_R t_p$ where t_p is the pulse duration. In the following, let us estimate the Rabi frequencies of the pulses employed in the experiment.

In the discrete levels of SF_6 where we know the oscillator strength quite well, we can easily estimate the Rabi precession frequency which determines the up pumping rate and the power broadening. For example, for a 0.1 J/cm^2, 30 psec pulse, $\omega_R \sim 33\ cm^{-1}$. However, in the QC, the oscillator strength is smeared out due to intermode coupling and intramolecular damping.[24] phenomenologically, we assume that the spread of oscillator strength is given by $1/\pi T_2$ where T_2 is the intramolecular relaxation time. The intramolecular relaxation time has been put within the limits of 30 psec and 0.7 psec recently by Kwok et al.[15] Therefore, the spread of the oscillator strength is within 0.3 cm^{-1} and 14 cm^{-1}. For the sake of giving a numerical example, let us take T_2 to be 5 psec so that the oscillator strength is spread over 2 cm^{-1}. We also make the assumption that the oscillator strength in the QC is simply reduced by the ratio of the laser linewidth and the width of the oscillator strength spread. Then the Rabi frequency for the same pulse mentioned above will become 6 cm^{-1}. Therefore, the area of the pulse is larger than unity invalidating Fermi's golden rule. Moreover, ω_R is comparable to the dephasing time T_2. This numerical example shows that for the picosecond CO_2 pulses at high intensities, the Rabi frequency is comparable in value to $1/\pi T_2$, i.e., the up-pumping rate of the system is comparable to or faster

than the intramolecular relaxation rate. This may be the reason why we observed an intensity dependent energy absorption.

There is no contradiction between this last conclusion and the fact that the absorbed energy is completely randomized during the laser pulse.[15] The up-pumping rate ω_R can be faster than the dephasing rate $1/T_2$ while T_2 can be shorter than the pulse duration. Moreover, we note that this occurs because of the very high laser intensities in the picosecond pulses. Our result does not necessarily mean that the energy absorption in the QC depends on the intensity even with ordinary nanosecond TEA CO_2 pulses. For those pulses, energy fluence should dominate over intensity dependent effects because the intensities are not high enough to overcome the T_2 intramolecular energy relaxation.

The thermal curve (e) in Fig. 7 represents the case of truly thermal multiphoton heating. Inasmuch as energy fluence scaling holds and intramolecular energy transfer is fast enough that only heat bath excitation[25] is important, all experimental $\langle n \rangle$ versus fluence curves should merge with the thermal curve at high intensities. We have shown above that this is not true for high peak power pulses. But with a molecule where the discrete level effects are not important, one should obtain better agreement between laser MPA and thermal heating. This was actually demonstrated by Cox and Horsley[26] in a complex molecule.

In summary, using picosecond pulses, we have experimentally demonstrated the case of truly nonthermal excitation of the SF_6

molecule, where the nonthermality does not merely come from bottlenecking effects. Instead it is due to the coherent nature of the laser-molecule interaction within the quasicontinuum.

(b) SF_6 at 650°K

In this experiment, we used the P(28) line of the laser. A fixed fluence (0.054 J/cm^2) truncated pulse of 30 nsec duration was used to preheat the SF_6 molecules as described in Section IV. A 50 psec pulse was then used to obtain the $\langle n \rangle$ versus fluence curve for the hot molecules using the procedure as described in Section III. In this experiment, we were not so much interested in the pulse duration dependence of $\langle n \rangle$ as the saturation properties of the QC. Therefore, only one laser pulse duration was used. Since all saturation phenomena are closely related to the relaxation mechanisms, a study of the saturation properties of the QC should provide some information on the intramolecular energy relaxation rate.

Figure 9 presents the measured energy deposition curve using 50 psec pulses with a 38.1 mm focal length germanium lens. A gas cell of 1 mm thickness containing 30 torr of SF_6 was used in this experiment. The experiment has been repeated several times and also different focal length lenses were used to make sure the results were reproducible. The spatial correction as described in Section III has already been applied in Fig. 9.

From the experimental data, one can also obtain the absorption cross-section σ of the preheated molecule as a function of the

laser fluence. Combining this curve with Fig. 9, one can then get the absorption cross-section as a function of internal energy in the molecule. This is shown in Fig. 10. On the same figure, we also plotted the thermal absorption data of Nowak and Lyman using a procedure as described in Appendix I.

From Fig. 10 we notice an initial saturation of absorption at low picosecond pulse fluences which seems to be universal for all polyatomic molecule MPA experiments. However, the absorption cross section rapidly approaches that of a thermally excited molecule at a moderate level of excitation of $\langle n \rangle \sim 8$. Unfortunately, the thermally measured data does not extend beyond 8.5 CO_2 photons of internal energy. However, comparing with a thermal band countour calculation,[27] represented as a dashed line in Fig.10, we can see that at higher values of $\langle n \rangle$, the observed absorption cross-section of the molecule is definitely larger than the value predicted with a thermal distribution of excitations. This is in agreement with the results obtained with 300°K SF_6 molecules in the previous section. It is further evidence that the nonthermal behavior of the SF_6 molecules does not come from the initial discrete levels, but rather is a property of the QC at such high laser intensities. The experimental values at high $\langle n \rangle$ have quite big error bars on them because they have the most experimental uncertainty and also the largest correction factors.

Let us estimate here whether 650°K is hot enough for the molecules to be considered in the QC. A heuristic definition of the QC is that

the power broadening introduced by the laser is sufficient to bring about an overlap of all the resonant lines of the system or

$$\omega_R \gg 1/\rho(E) \tag{10}$$

where $\rho(E)$ is the density of states of the molecule. This operational definition of the QC depends on the experimental situation and is therefore not universally applicable. In particular, it is easily satisfied by the picosecond pulses because of their large Rabi precession frequencies and power broadening. For SF_6 at 650°K, $\rho(E) \sim 10/cm^{-1}$.[6(c)] The power broadening for the lowest data point in Fig. 9 is estimated to be ~1 cm^{-1}. Hence the QC condition is satisfied. However, it is expected that for a thermal distribution of population at 650°K, there must be still some molecules trapped in the initial discrete levels. This presumably is the cause of the initial saturation of absorption in Fig. 10. To alleviate this problem and perform a cleaner experiment on the QC, one can either preheat the molecule with a stronger prepulse, or use a picosecond pulse for preheating, or use overtone pumping by a strong dye laser.

The thermal curves used in Figs. 7 and 10 should only be regarded as a reference. Since no simple statistical definition of temperature exists for a molecule under MPA pumping conditions, it is unfair to claim that SF_6 should behave as if an equilibrium Boltzmann population distribution has been achieved.

Figure 10 represents the saturation of absorption in the QC. All previous measurement of this phenomenon had blended into a great extent the effects of the discrete level bottleneck. As mentioned above, the observed absorption can be called "superthermal" because it is always larger than the thermal absorption at the same internal energy. Stone and Goodman[28] recently pointed out a new formulation of the absorption in the QC using a fully coherent interaction picture. They showed that energy deposition and hence the absorption cross section can be intensity dependent if the radiative pumping time scale is comparable to the intramolecular relaxation time. This also was pointed out by Quack[20c] in deriving the master rate equations from the Schrodinger equation describing the laser-molecule interaction. Multiphoton interaction in polyatomic molecules using very strong laser fields and short pulse durations is characteristically different from ordinary TEA laser interactions and merits much more careful investigation, both experimentally and theoretically.

While the observation can be explained qualitatively, a thorough understanding of the role of intensity is still lacking. Especially the population distribution and the possible multilevel coherence still need to be studied and clarified.

Notice that there are two types of dephasing of the coherent state prepared by the CO_2 laser. The T_2 type intramolecular relaxation couples the energy into the heat bath. This dephasing conserves the energy in the molecule. The other kind of dephasing arises from the

inhomogeneous broadening of the ν_3 band. The laser pulse will excite simultaneously states that are within the linewidth $\Delta\nu_L$ of the laser. They will beat together incoherently and dephase the coherence[23] in a time $1/\Delta\nu_L$ which is simply the laser pulse duration. This type of dephasing is responsible for the adiabatic decay observed by Kwok et al. Recently Steel et al.[29] observed a collisionless dephasing of the $2\nu_3$ level using degenerate form wave mixing of 1.8 nsec. Since 1 nsec pulses were employed, their results were probably due to the second type of dephasing which has nothing to do with intramolecular energy relaxation, contrary to the interpretation by Galbraith et al.[20a]

VII. CONCLUSION

In this paper we have described two measurements of MPA in SF_6 using picosecond CO_2 laser pulses. We found that for such pulses, the energy fluence scaling law no longer holds. Instead, a remarkable intensity dependence was observed. This effect is inherent with the picosecond pulses because (i) the corresponding intensities and Rabi frequencies are high, comparable or larger than the intramolecular relaxation rate of the molecule, and (ii) the transform limited lifetime broadening of these pulses enables the coupling of more states in the QC. Thus, the reduced oscillator strength as discussed by Goodman et al.[24] is no longer very small, as in the case of ordinary TEA CO_2 pulses.

Although energy fluence scaling has played an important role as a zeroth order approximation in the description of multiphoton dissociation, the limitations of its validity must be recognized. For picosecond pulses the Rabi frequency can readily be increased to levels where the one-photon rate equations for QC absorption have to be modified by coherent effects. It is also well known that at small Rabi frequencies bottlenecking effects are important. This occurs for pulses of 0.1 J/cm^2 or less with deviations of more than one nanosecond. In both cases intensity dependent effects are observed which depend on the pulse duration at constant energy fluence. Although it is difficult to vary the pulse duration at constant fluence over many orders of magnitude, more experiments on absorption of picosecond pulses by other molecules are desirable. The

dissociation probability by a pulse of fixed picosecond duration should also be measured as a function of intensity. It is believed that picosecond data can test more precisely various theoretical models of excitation in the QC regime.

Although it is possible to achieve a nonthermal population distribution by picosecond pumping, no claim for mode selective chemistry is made. Energy equipartition will occur rapidly, albeit in a time longer than the Rabi period. It is believed that molecules can be excited to energies considerably higher than with longer pulses. This should be observable as an increase in the internal and kinetic energies of dissociation products in molecular beam experiments.

One of us (HSK) wishes to thank Professors Y. T. Lee and Y. R. Shen for helpful discussions. This research was supported by Joint Services Electronics Program under Contract No. N00014-75-C-0648 and by ONR under Contract No., N00014-78-C-0531.

APPENDIX I. THERMAL MPA IN SF_6

In this appendix, we explain how the thermal curves in Fig. 7 and Fig. 10 were obtained from the thermal shock tube measurements of Nowak and Lyman.[18] They basically measured the small signal absorption cross section σ of an excited SF_6 molecule at T°K. Now, using quantum statistics, it is possible to relate the total internal energy in the molecule E and the temperature T. The average number of photons $\langle n \rangle$ deposited is related to E by

$$E = E_0 \text{ (at } 300^\circ K) + \langle n \rangle \hbar\omega \tag{11}$$

Therefore, from the NL data of σ versus T, we can obtain a curve of σ versus $\langle n \rangle$ for both the P(20) and P(28) lines of the CO_2 laser. This was the smooth curve in Fig. 10.

The next step involves the reduction of the data to get the $\langle n \rangle$ versus fluence J. This is the hypothetical energy deposition curve if the absorption of the molecule follows the thermal cross-section. Note that

$$\sigma = \frac{d\langle n \rangle}{dJ} \hbar\omega \tag{12}$$

can be written as

$$\hbar\omega \frac{1}{\sigma} d\langle n \rangle = dJ$$

Integrating both sides from the initial condition $\langle n \rangle = 0$ at $J = 0$, gives

$$\hbar\omega \int_0^{\langle n \rangle} \frac{1}{\sigma} \, d\langle n \rangle = J$$

Since σ has already been reduced to be a function of $\langle n \rangle$, the integral on the left-hand-side can be evaluated numerically with the upper limit as a parameter. Thus one can obtain a curve of $\langle n \rangle$ versus J as in Fig. 7.

REFERENCES

1. (a) N. Bloembergen and E. Yablonovitch, Phys. Today, May 1978, p.23; (b) P. A. Schulz, Aa. S. Sudbo, D. J. Krajnovich, H. S. Kwok, Y. R. Shen, and Y. T. Lee, Ann. Rev. Phys. Chem. 30, 379 (1979); (c) J. P. Aldridge III, J. H. Birely, C. D. Cantrell, and C. D. Cartwright, in Physics of Quantum Electronics, Vol. 4, ed. S. F. Jacobs, M. Sargeant III, M. D. Scully and C. T. Walker, Addition-Wesley, Reading, Ma. (1980).

2. H. -L. Dai, A. H. Kung, and C. B. Moore, Phys. Rev. Lett. 43, 761 (1979).

3. (a) J. G. Black, E. Yablonovitch, E. Bloembergen and S. Mukamel, Phys. Rev. Lett. 38, 1131 (1977); (b) J. G. Black, P. Kolodner, M. J. Schultz, E. Yablonovitch and N. Bloembergen, Phys. Rev. A19, 701 (1979).

4. D. J. Krajnovich, A. Giardini-Guidoni, Aa. S. Sudbo, P. A. Schulz, Y. R. Shen, and Y. T. Lee, paper presented at the European Physical Society Conference, Heriot-Watt University, Edinburgh, Scotland (1978).

5. (a) Aa. S. Szabo, D. J. Krajnovich, P. A. Schulz, Y. R. Shen, and Y. T. Lee, in Multiphoton Excitation and Dissociation of Polyatomic Molecules, C. D. Cantrell, ed., Springer-Verlag, New York (1979); (b) F. Brunner and D. Proch, J. Chem. Phys. 68, 4936 (1978).

6. (a) H. S. Kwok and E. Yablonovitch, Rev. Sci. Instr. 46, 814 (1975); (b) H. S. Kwok, Ph.D. Thesis, Harvard University (1978).

7. R. L. Shoemaker, Ann. Rev. Phys. Chem. 30, 239 (1979).

8. H. S. Kwok and E. Yablonovitch, Opt. Comm. 21, 252 (1977).

9. A. Gondhalekar, N. R. Heckenberg and E. Holzhauer, IEEE JQE 11, 103 (1975).

10. H. S. Kwok and E. Yablonovitch, Appl. Phys. Lett. 27, 583 (1975).

11. E. Yablonovitch and J. Goldhar, Appl. Phys. Lett. 25, 580 (1974).

12. E. T. Gerry and D. A. Leonard, Appl. Phys. Lett. 8, 227 (1966).

13. H. S. Kwok, to be published in J. Appl. Phys.

14. (a) D. O. Ham and M. Rothschild, Opt. Lett. 1, 28 (1977); (b) T. F. Deutsch, Opt. Lett. 1, 25 (1977).

15. H. S. Kwok and E. Yablonovitch, Phys. Rev. Lett. 41, 745 (1978).

16. P. Kolodner, H. S. Kwok, J. G. Black and E. Yablonovitch, Opt. Lett. 4, 38 (1979).

17. (a) J. I. Steinfeld, I. Burak, A. V. Nowak, and D. G. Sutton, J. Chem. Phys. 52, 5421 (1970); (b) J. T. Knudtson and G. W. Flynn, J. Chem. Phys. 58, 1467 (1972).

18. A. V. Nowak and J. L. Lyman, J. Quant. Spect. Rad. Transf. 15, 945 (1975).

19. The communications of the most recent and accurate data presented in Fig. 7 by J. G. Black is gratefully acknowledged.

20. (a) H. W. Galbraith and J. R. Ackerhalt in Laser Induced Chemical Processes, Vol. I, ed. J. I. Steinfeld, Plenum Press, 1980; (b) D. Hodgkinson and J. Briggs, Chem. Phys. Lett. 64, 511 (1979); (c) M. Quack, J. Chem. Phys. 69, 1282 (1978).

21. P. A. Schulz, Ph.D. Thesis, University of California, Berkeley (1979).

22. E. Merzbacher, Quantum Mechanics, Wiley, New York, 1961.

23. L. Allen and J. H. Eberly, Optical Resonance and Two-Level Atoms, Wiley, New York (1975).

24. M. Goodman, J. Stone, and D. Dows, J. Chem. phys. 65, 5052 (1976).

25. E. Yablonovitch, Opt. Lett. 1, 87 (1977).

26. D. M. Cox and J. A. Horsley, J. Chem. Phys. 72, (864 (1980).

27. R. S. Taylor, T. A. Znotin, E. A. Ballik, and B. K. Garside, J. Appl. Phys. 48, 4435 (1977).

28. J. Stone and M. F. Goodman, J. Chem. Phys. 71, 408 (1979).

29. D. G. Steel and J. F. Lam, Phys. Rev. Lett. 43, 1588 (1979).

30. Incidentally, the experiment curve in Fig. 8 together with the thermal limit asymtote can be used to estimate the fraction of molecules "trapped" in the discrete levels as a function of laser intensity. If the fraction of molecules pumped to the QC is defined by $\langle n \rangle / \langle n \rangle_{th}$ where $\langle n \rangle_{th} = 11.5$ for this particular case, then the results obtained will agree quite well with that of Reference 21. The latter estimate is also collaborated by the photoionization data on SF_6. See Aa. S. Sudbo, P. A. Schulz, D. J. Kragnovich, Y. T. Lee and Y. R. Shen, Opt. Lett. 4, 219 (1979).

31. From the onset of coherent interaction, one can estimate crudely the magnitude of the dephasing time T_2. Assume that $\mu_{eff}E/ \approx 1/\pi T_2$ at the onset. As discussed in the text, the effective transition moment is given by $\mu_{eff} = \mu(\Delta\nu_L/\Delta\nu_H)$ where $\Delta\nu_L$ is the laser linewidth and $\Delta\nu^H \approx 1/\pi T_2$. If coherent effect starts to compete with intramolecular dephasing at 400 MW/cm^2, then the above argument gives $T_2 \sim 6.6$ psec, which is not unreasonable.

FIGURE CAPTIONS

Fig. 1. The picosecond CO_2 laser system. A fast oscilloscope is used to monitor the zeroth order output of the grating. The output mirror of the CO_2 laser is translatable by a double differential micrometer for the adjustment of the cavity length. This procedure guarantees a single longitudinal mode output at all times. The d.c. spark gap is formed by two sharp points on a carbonized surface and is placed at 2 mm from the focal point of the plasma shutter.

Fig. 2. Experimentally measured absorption coefficient of the TEA laser pulse by the hot CO_2 molecules as a function of gas tube pressure. The CO_2 gas was heated to 700°K. Two separate regions of Doppler and pressure broadening can clearly be distinguished.

Fig. 3. Experimental setup for the measurement of the transmission of the picosecond CO_2 laser pulse as a function of pulse intensity. A second preheating truncated pulse channel is also shown. The Ge:Au detector was placed inside a copper box for shielding from electromagnetic noise.

Fig. 4. SF_6 absorption cross-section at P(20) under collisional laser excitation. 30 nsec long truncated CO_2 laser pulse was used.

Fig. 5. A measurement of the absorption cross-section at P(28) showing the achievement of thermal heating of the SF_6 molecules by collisional multiphoton absorption. Experiment was done with a truncated pulse, followed by a picosecond probe pulse with 32 nsec time delay.

Fig. 6. Energy deposition $\langle n \rangle$ as a function of the laser fluence for four different picosecond pulse durations. As explained in the text, no dissociation can occur during the pulse interaction even at $\langle n \rangle > 40$.

Fig. 7. Energy deposition curves $\langle n \rangle$ at P(20) for various pulse conditions (a) 30 psec date from this experiment, (b) 500 psec data from Ref. 19, (c) 30 nsec data from Ref. 19, (d) 100 nsec data from Ref. 19, (e) derived thermal absorption data from Ref. 18.

Fig. 8. Energy absorbed by the SF_6 molecule as a function of pulse intensities at a fixed energy fluence of 0.2 J/cm^2. The dashed line indicates the expected behavior if energy absorption in the QC depends only on pulse fluence. The asymtotic value of $\langle n \rangle$ is obtained from Nowak and Lyman's data (Ref. 18).

Fig. 9. Energy deposition $\langle n \rangle$ as a function of pulse fluence. 50 psec P(28) CO_2 laser pulses were used. SF_6 cell pressure was 30 torr and preheated to 650°K before the picosecond pulse arrived.

Fig. 10. Absorption cross section σ as a function of internal energy of the SF_6 molecules at the p(28) line of the CO_2 laser. Data became more inaccurate at high energies. Solid curve shows the thermal data from Ref. 18, dotted line is the theoretical calculation from Ref. 26.

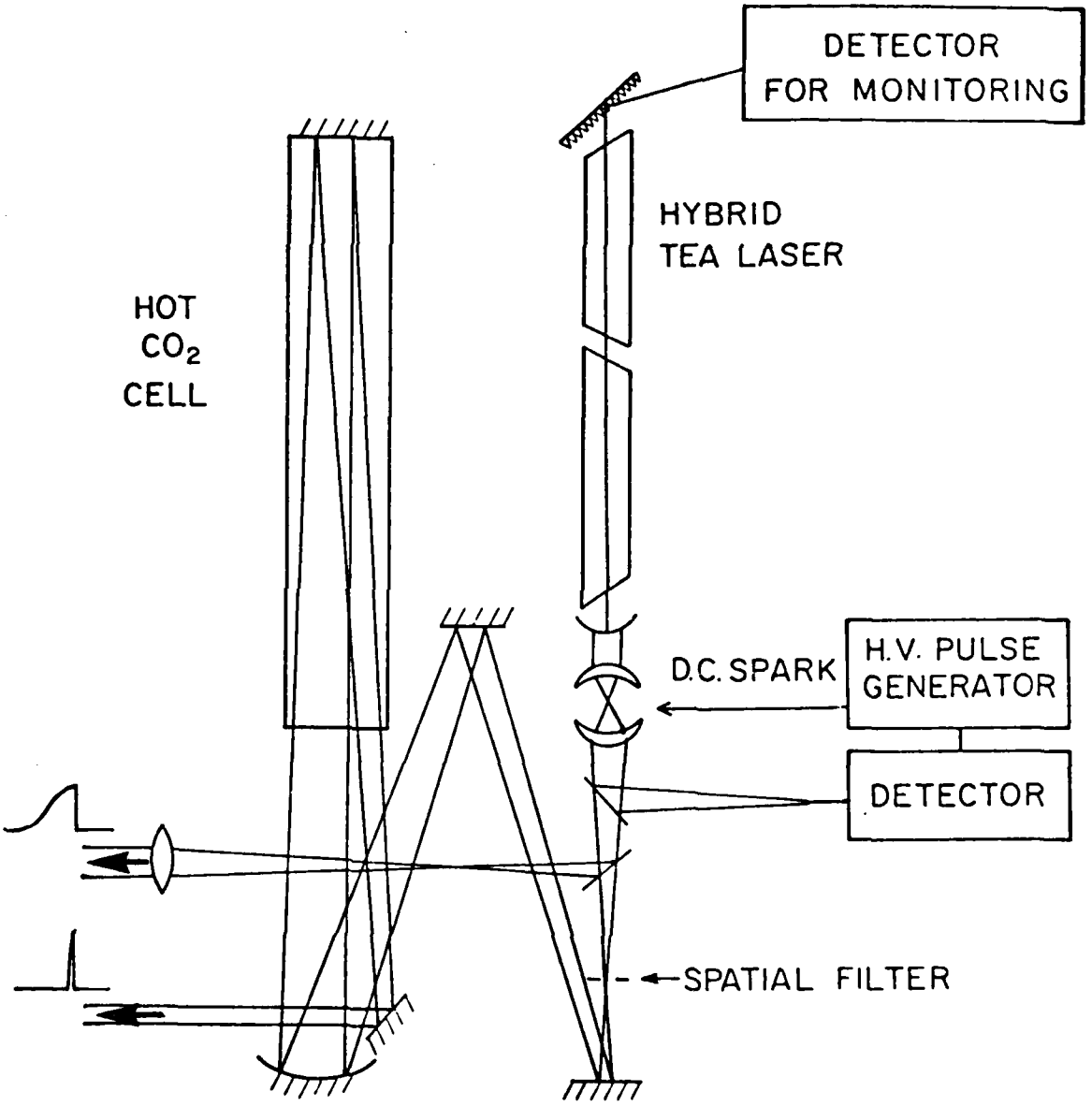
DETECTOR
FOR MONITORING
HYBRID
TEA LASER
HOT
CO_2
CELL
D.C. SPARK
H.V. PULSE
GENERATOR
DETECTOR
SPATIAL FILTER

Figure 1

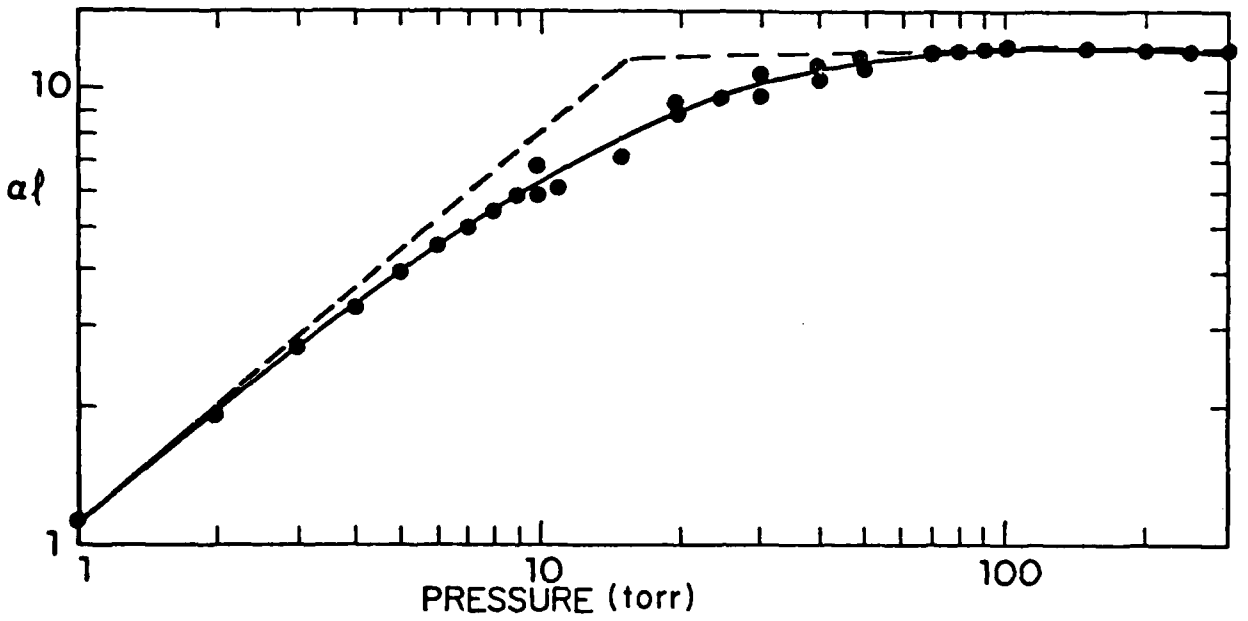

Figure 2

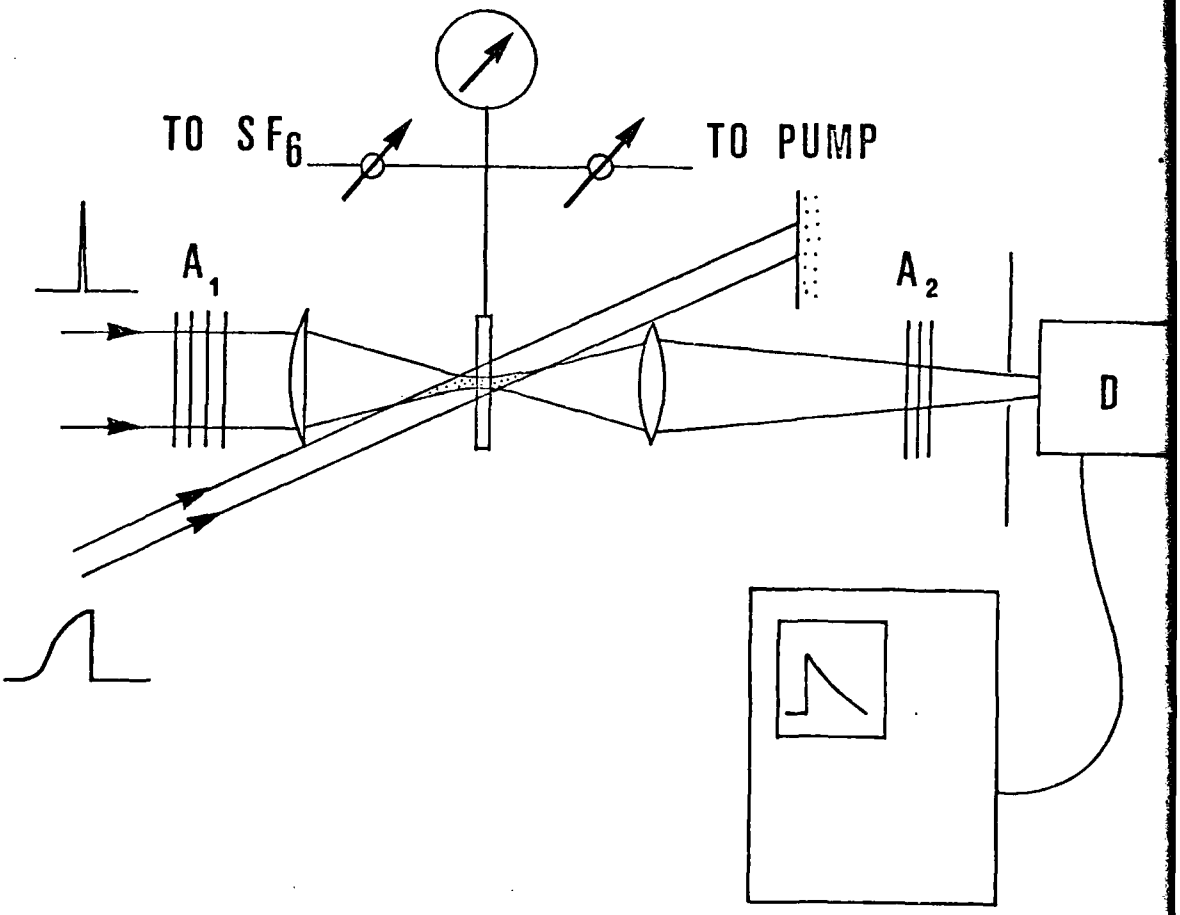

Figure 3

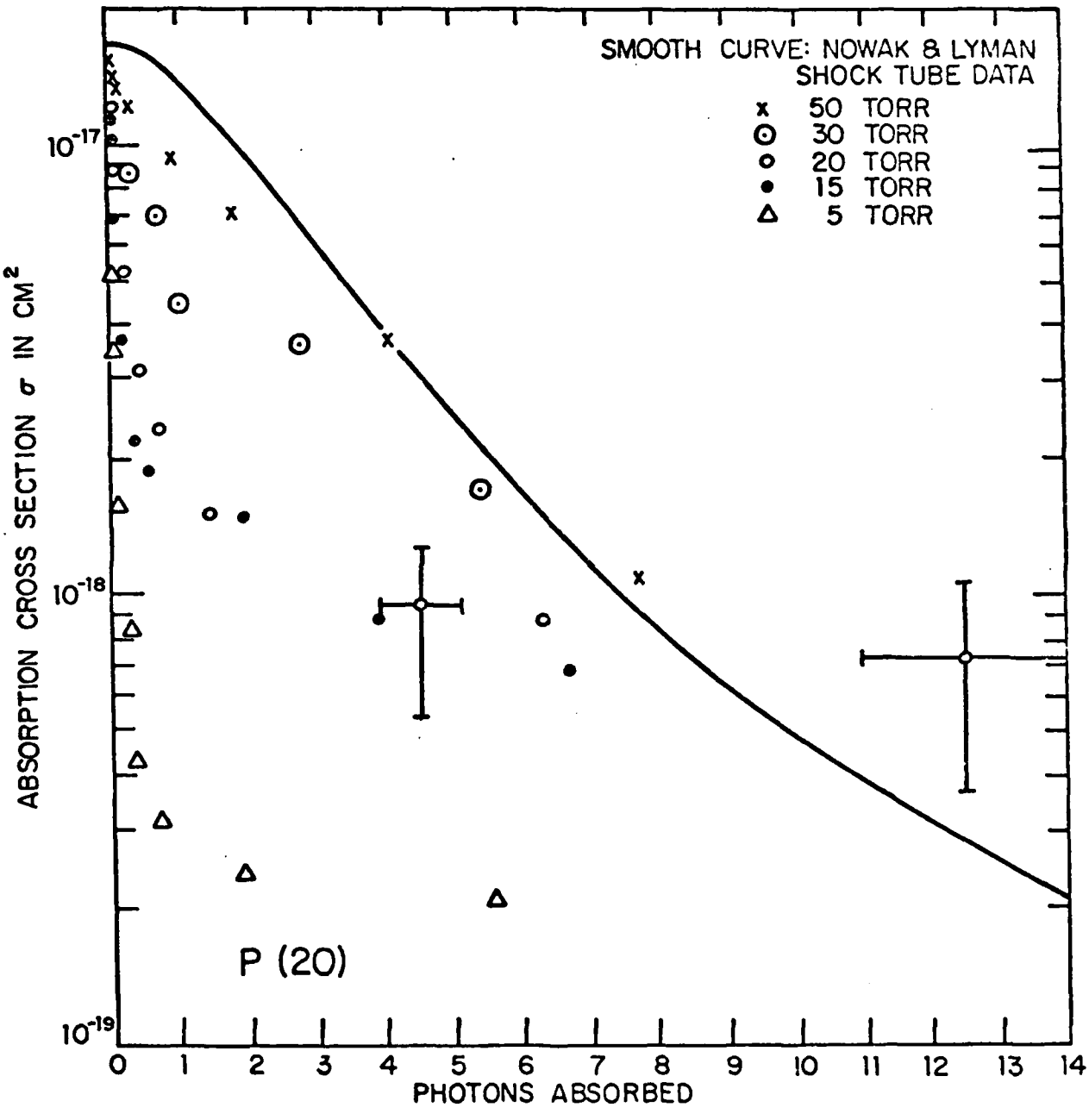
SMOOTH CURVE: NOWAK & LYMAN
SHOCK TUBE DATA
50 TORR
30 TORR
20 TORR
15 TORR
5 TORR
ABSORPTION CROSS SECTION σ IN CM²
10⁻¹⁷
10⁻¹⁸
10⁻¹⁹
P (20)
0 1 2 3 4 5 6 7 8 9 10 11 12 13 14
PHOTONS ABSORBED

Figure 4

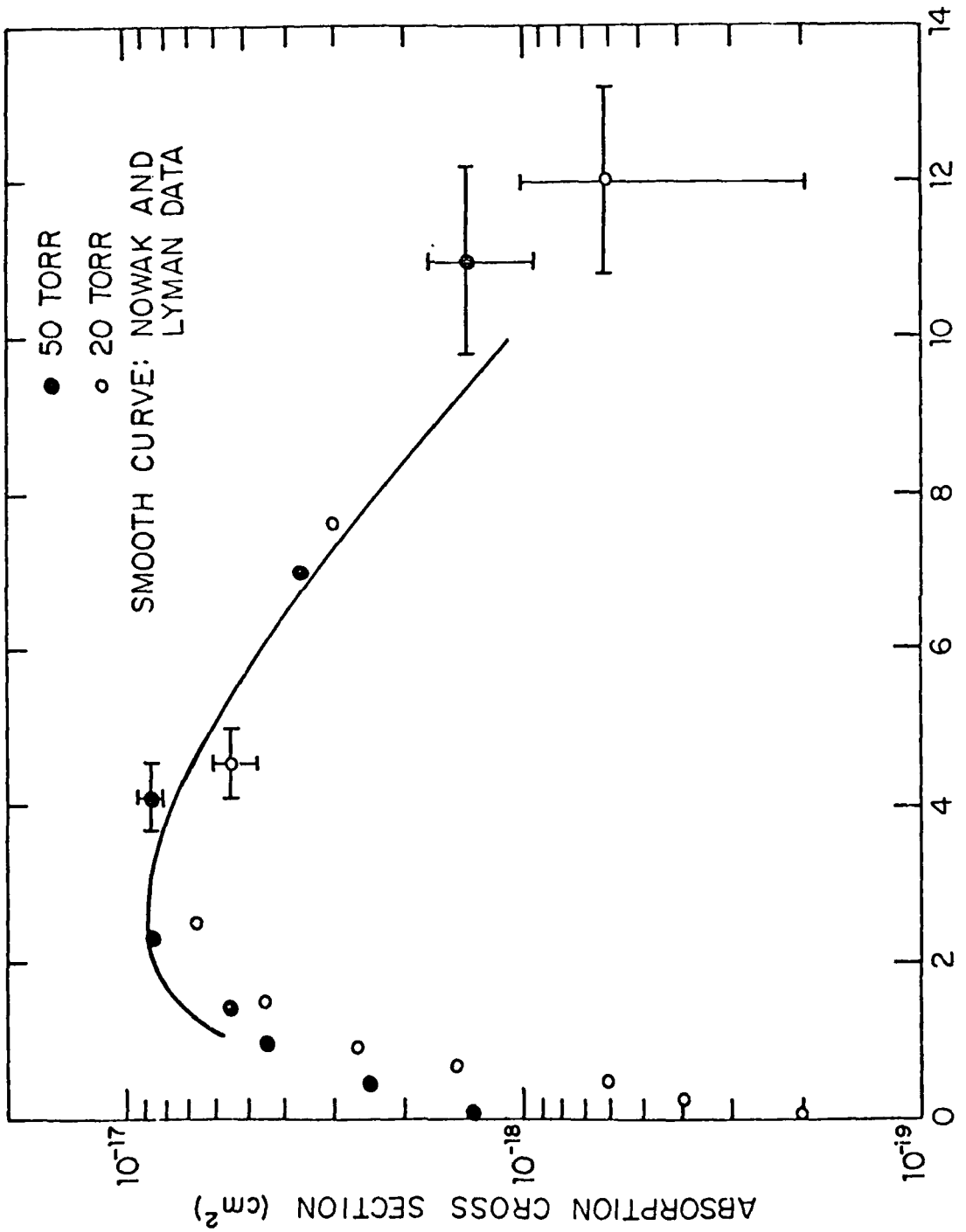
ABSORPTION CROSS SECTION (cm²)
10⁻¹⁷
10⁻¹⁸
10⁻¹⁹
PHOTONS ABSORBED
0
2
4
6
8
10
12
14
● 50 TORR
○ 20 TORR
SMOOTH CURVE: NOWAK AND LYMAN DATA

Figure 5

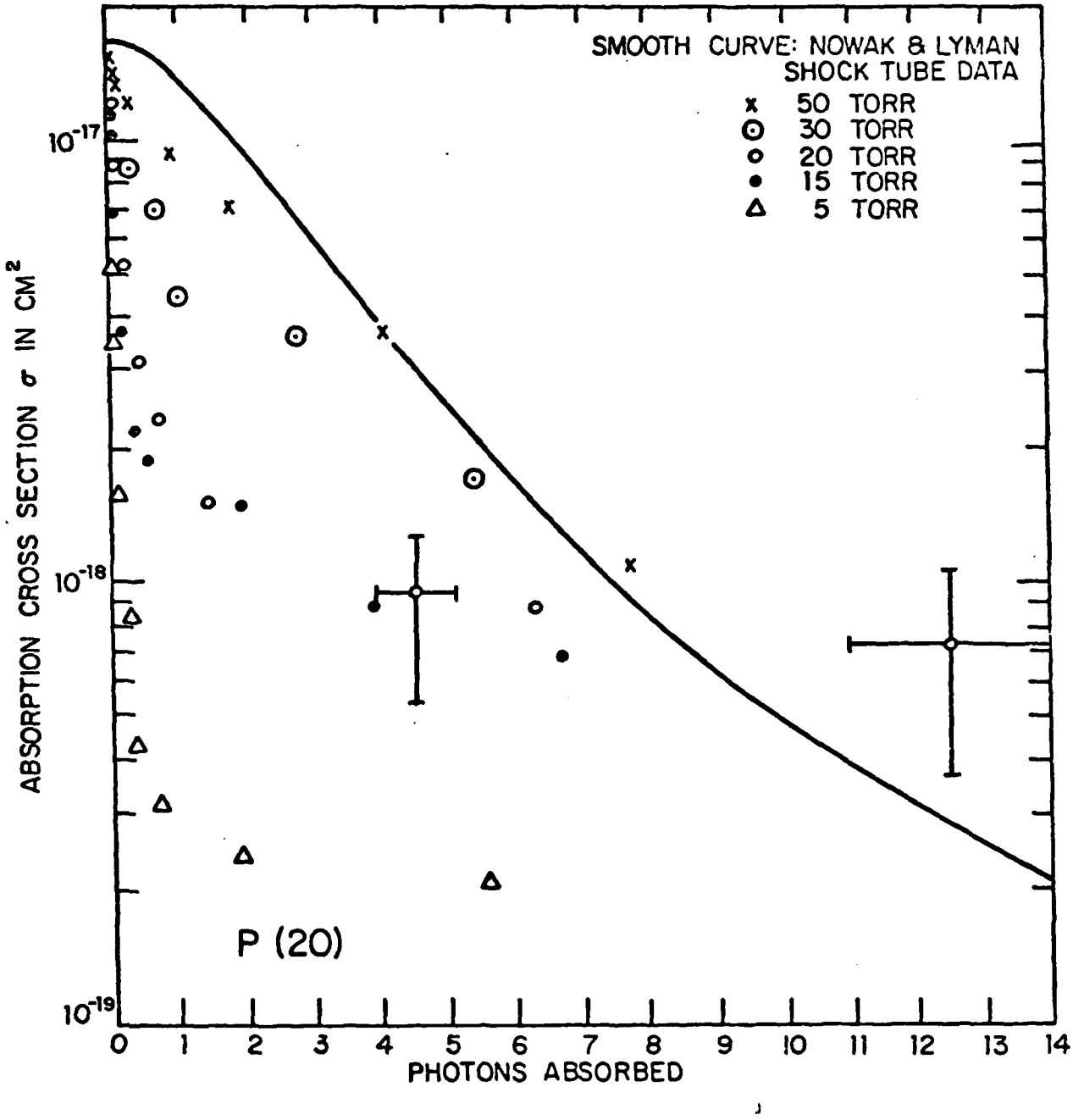
SMOOTH CURVE: NOWAK & LYMAN
SHOCK TUBE DATA
50 TORR
30 TORR
20 TORR
15 TORR
5 TORR
ABSORPTION CROSS SECTION σ IN CM²
10⁻¹⁷
10⁻¹⁸
10⁻¹⁹
P (20)
0 1 2 3 4 5 6 7 8 9 10 11 12 13 14
PHOTONS ABSORBED

Figure 4

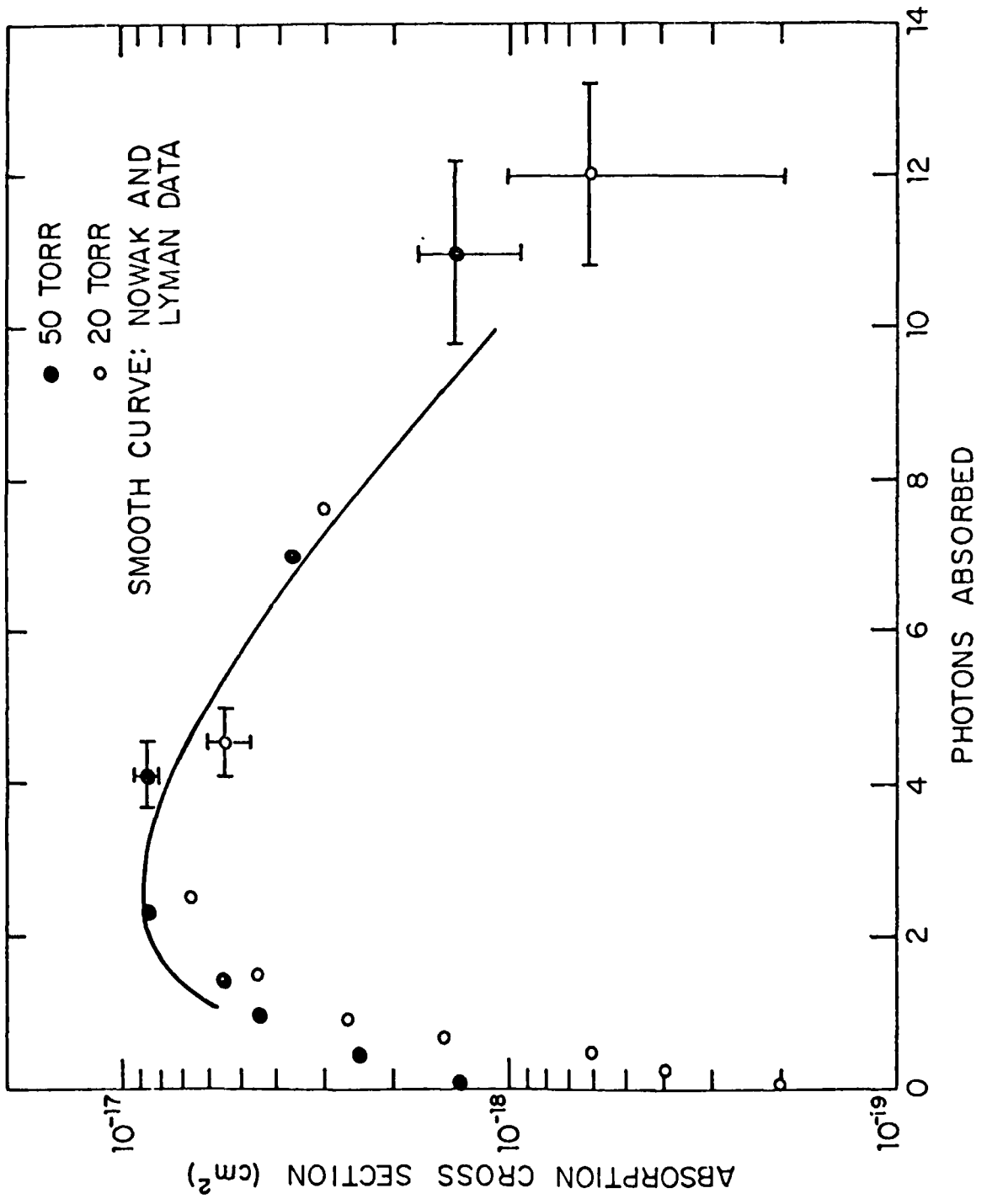
ABSORPTION CROSS SECTION (cm²)
10⁻¹⁷
10⁻¹⁸
10⁻¹⁹
PHOTONS ABSORBED
0
2
4
6
8
10
12
14
● 50 TORR
○ 20 TORR
SMOOTH CURVE: NOWAK AND LYMAN DATA

Figure 5

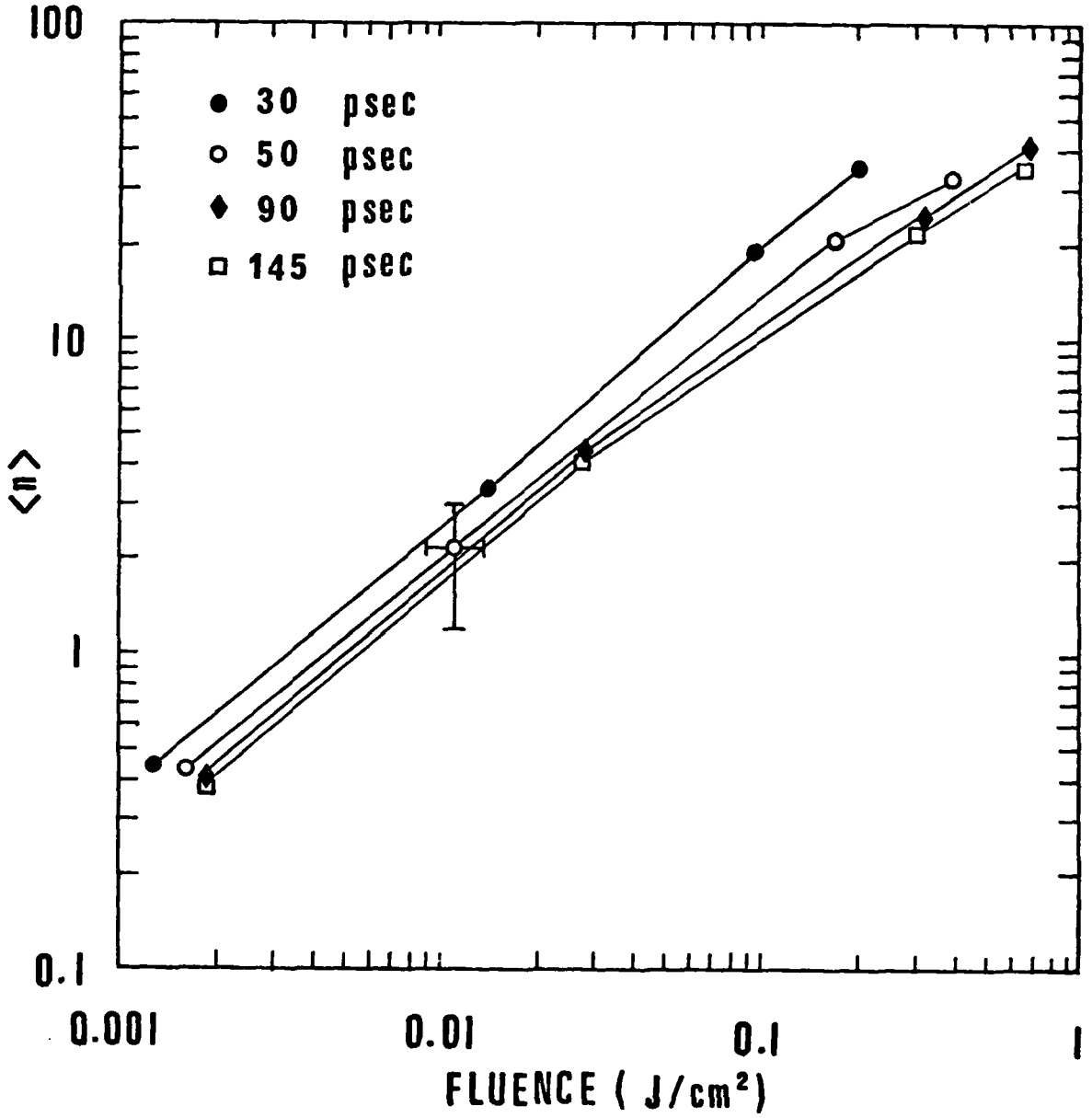
100
10
1
0.1
<n>
30 psec
50 psec
90 psec
145 psec
0.001
0.01
0.1
1
FLUENCE (J/cm²)

Figure 6

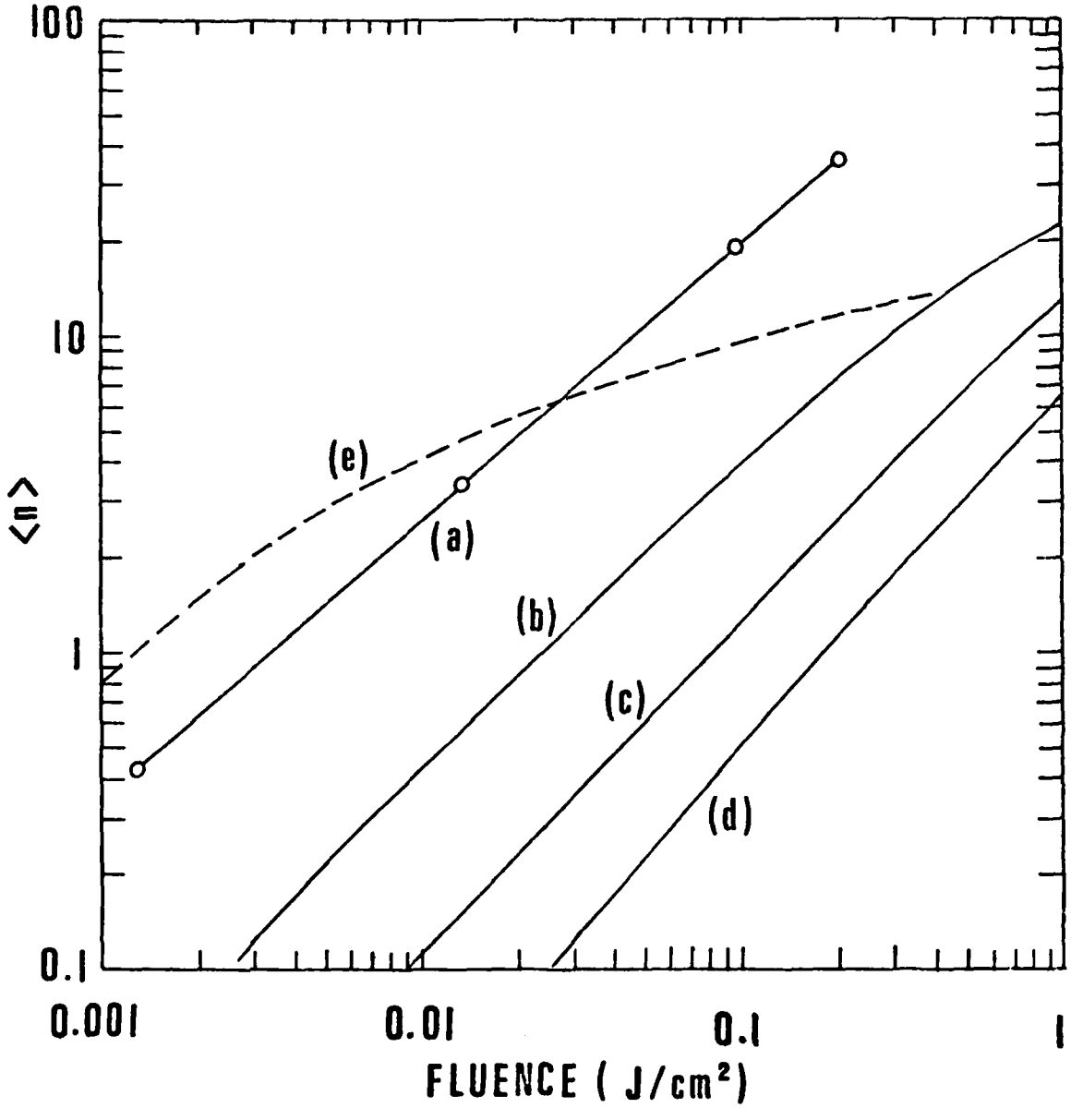

Figure 7

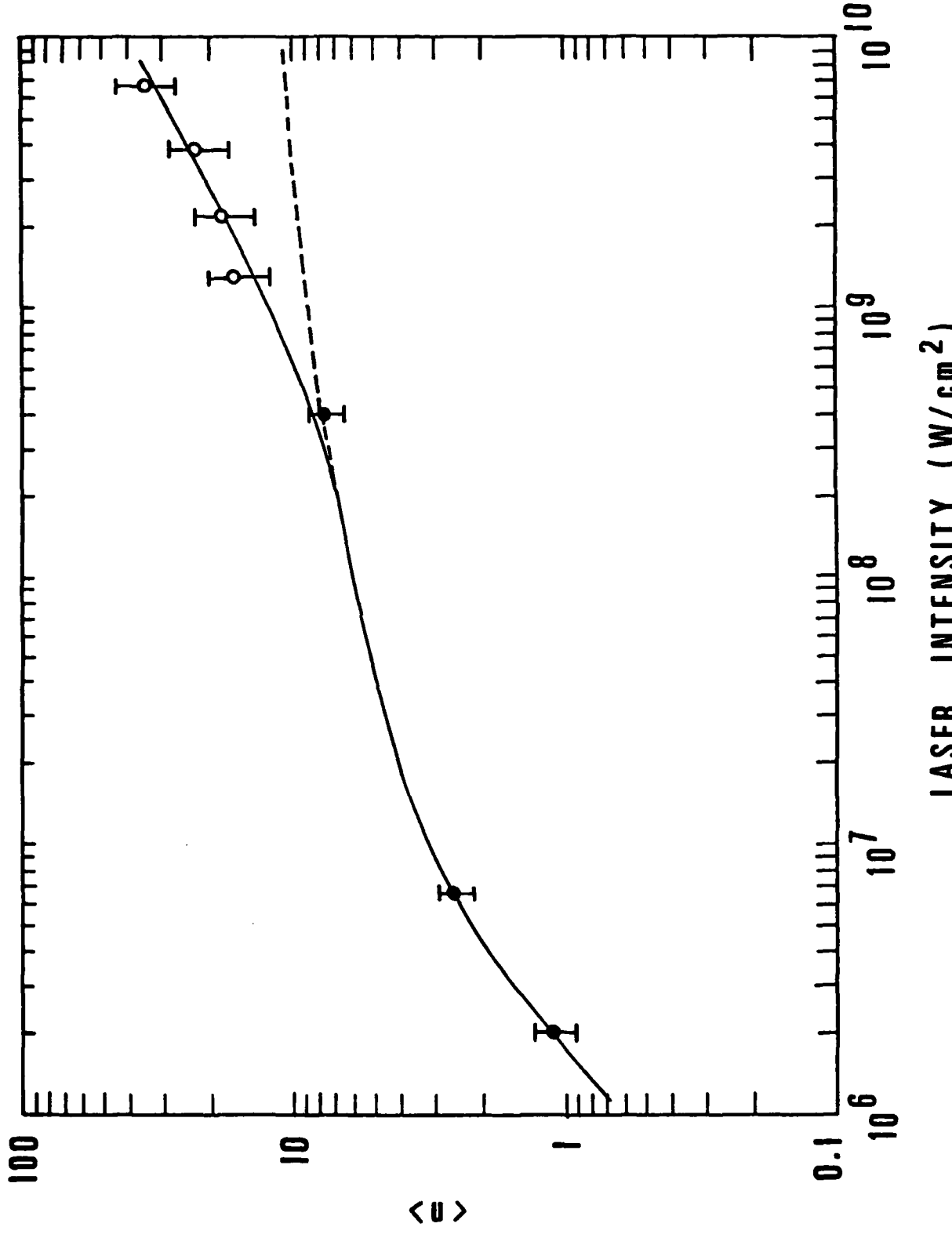

Figure 8

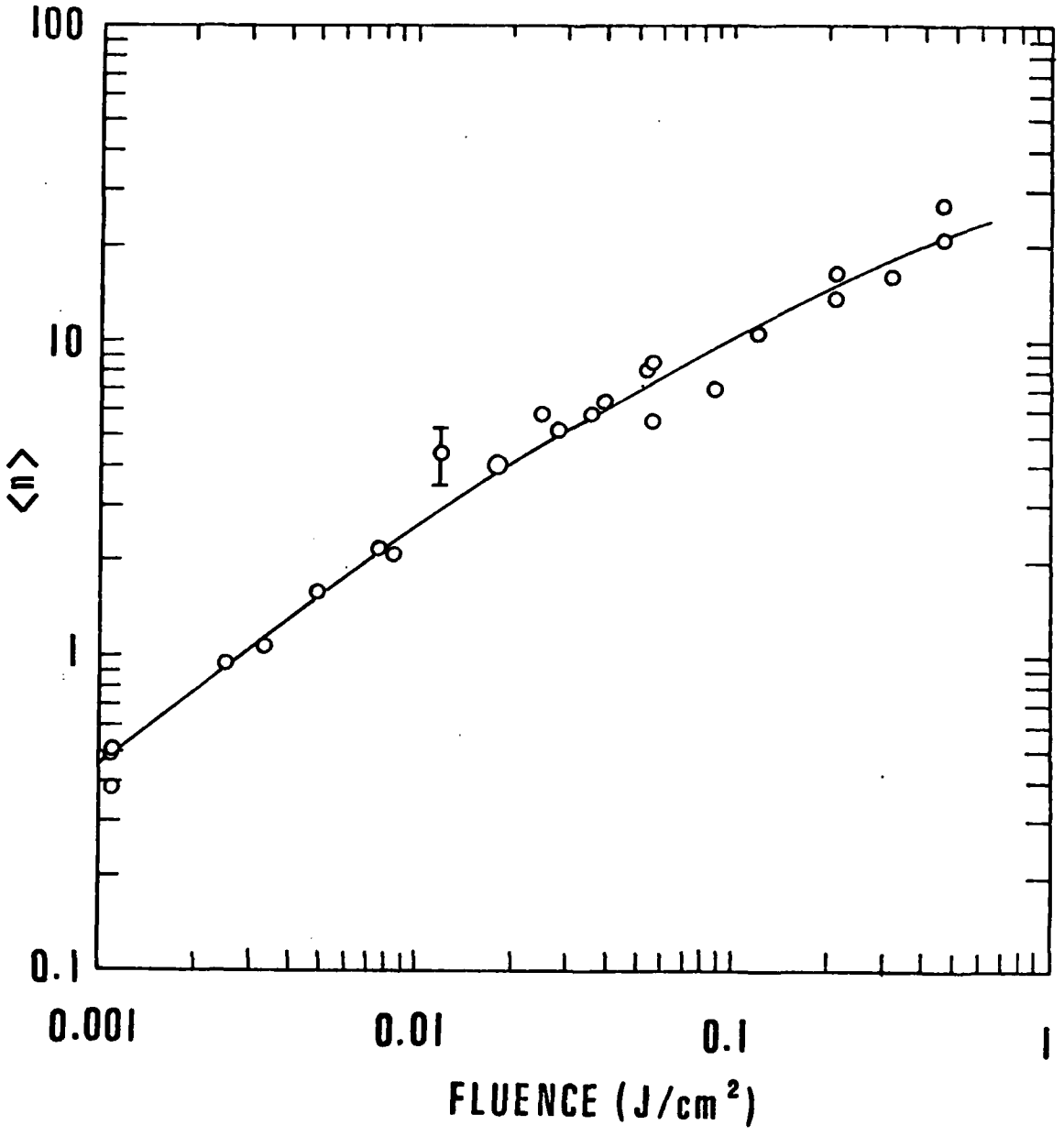

Figure 9

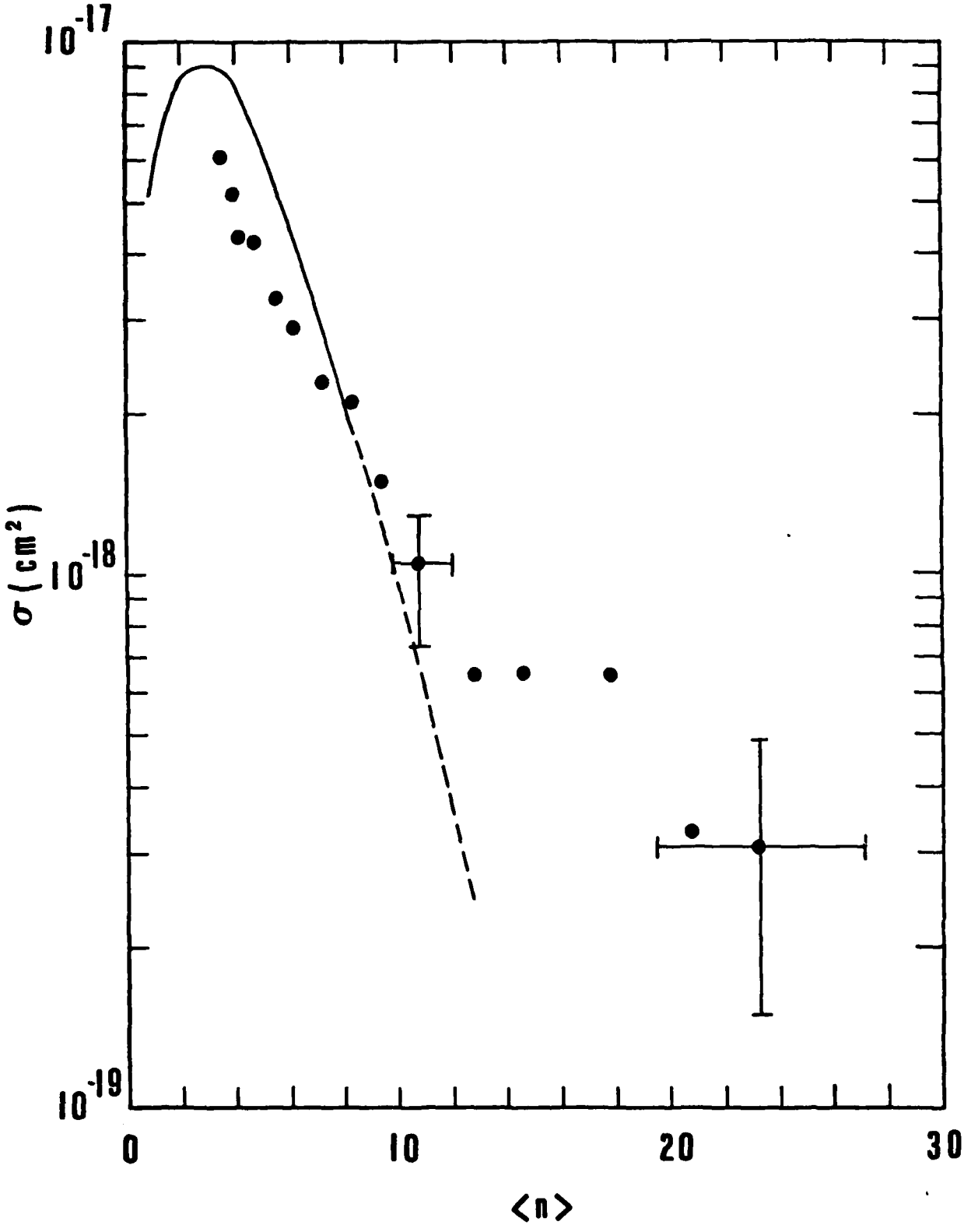

Figure 10

Volume 68, number 1 CHEMICAL PHYSICS LETTERS 1 December 1979

MULTIPHOTON VIBRATIONAL PUMPING OF OPTICALLY PREPARED NO_2 MOLECULES*

Itamar BURAK**, Jeffrey TSAO, Yehiam PRIOR‡ and Eli YABLONOVITCH
Gordon McKay Laboratory, Harvard University, Cambridge, Massachusetts 02138, USA

Received 6 September 1979

Reported is the collisionless infrared multiphoton excitation of NO_2 molecules initially prepared in an electronically excited state. From the shape of the infrared induced blue-shifted fluorescence spectrum the probability distribution $P(n)$ for the net absorption of n photons has been deduced.

The shape of the probability distribution function $P(n)$ for n-photon infrared excitation of molecules has been the subject of lively discussion in the literature [1–3]. In this work, we report the observation of infrared multiphoton vibrational excitation of a molecule initially prepared in an electronically excited state. By monitoring the transient visible fluorescence spectrum, we determined the energy distribution function produced by collisionless infrared multiphoton pumping.

Vibrational excitation of an electronically excited molecule has been reported earlier [4] for the ^3A_u state of biacetyl. That excitation involved a collisional energy exchange between vibrationally excited ground state molecules and optically prepared triplet molecules. The present experiment involves single photon optical excitation of NO_2 molecules from the $^2A_1$ ground state to high levels of the strongly mixed $^2B_2$–$^2A_1$ vibronic manifold, followed by direct infrared multiphoton pumping with a very short CO_2 laser pulse. This work was prompted by an earlier report [5], in which weak double resonance signals were observed in NO_2 molecules exposed simultaneously to cw Ar^+ and CO_2 laser beams.

The experimental arrangement is shown in fig. 1a.

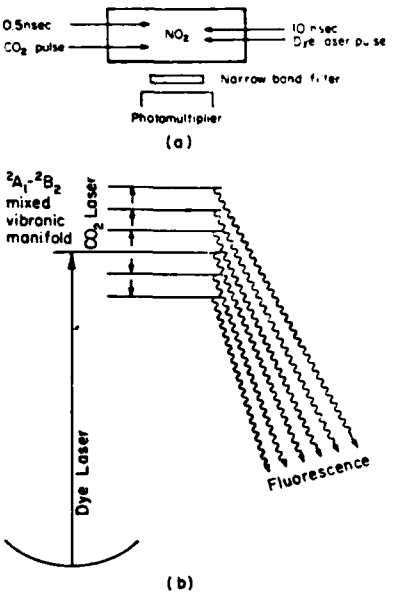

Fig. 1. (a) Schematic of the experimental arrangement. (b) Schematic diagram of pumped energy levels.

A gas cell of NO_2 at a pressure ≈ 250 mTorr is subjected to a 0.5 ns CO_2 laser pulse and an antiparallel 10 ns dye laser pulse which overlaps the central uniform intensity region of the infrared beam. The delay between the two pulses can be adjusted from 0–30 μs with a 30 ns jitter. The fluorescence pulse from the excited NO_2 molecules is imaged onto a photomultiplier tube through narrow bandpass filters

* Supported by Office of Naval Research.
** On leave from the Department of Chemistry, Tel Aviv University, Israel.
‡ Permanent address: Department of Chemical Physics, The Weizmann Institute, Rehovot, Israel.

and recorded on a dual-beam oscilloscope. Fig. 1b illustrates the energy levels participating in the experiment.

A typical series of fluorescence signals generated by the CO_2 laser *following* dye laser excitation is shown in fig. 2. A small portion of the scattered visible laser pulse leaked through the narrow band filter and was recorded at the left edge of the lower trace. The fluorescence pulse in the lower trace occurs at the instant of the delayed CO_2 pulse which is on the upper trace of fig. 2. As can be seen the amplitude of the generated fluorescence decreases at a characteristic rate k_0' as the delay between the two pulses increases. No signals are obtained when the infrared pulse *precedes* the visible pulse. While ordinary visible excitation leads only to Stokes-shifted fluorescence, CO_2 laser induced signals are detected at frequencies blue-shifted with respect to the dye laser frequency ω_0. The spectral width of the induced fluorescence depends on both the CO_2 laser's energy fluence and intensity. Fluorescence signals have been recorded at frequencies blue-shifted from ω_0 by energies up to 5 times the CO_2 photon energy. The induced fluorescence spectrum is shown in fig. 3.

The relaxation features exhibited by the multiphoton induced amplitude and fluorescence decays are comparable with the decays of ordinary fluorescence signals. Our study of the ordinary fluorescence

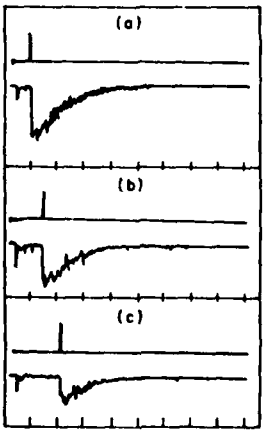

Fig. 2. Upper trace: infrared laser. Lower trace: induced fluorescence signal at 470 nm following dye laser excitation at 502 nm. Delays are (a) 250 ns, (b) 500 ns, (c) 750 ns. Time scale 500 ns/division.

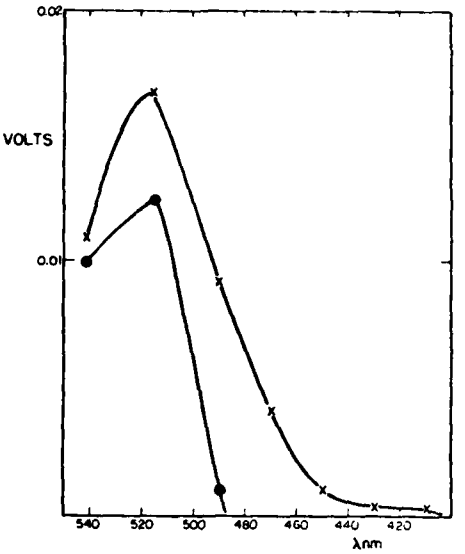

Fig. 3. Dots: ordinary fluorescence spectrum excited by dye laser at 502 nm. Crosses: prompt spectrum induced by CO_2 laser following dye laser excitation.

decay can be summarized as follows:

(a) The fluorescence decay times measured at pressures exceeding 100 mTorr scale inversely with the pressure.

(b) These decay times depend strongly on the observation frequency ω. When fluorescence is studied near the excitation frequency ($\omega_0 - \omega \approx 500$ cm^{-1}), a quenching rate $k_0 \approx 5.5 \times 10^6$ s^{-1} Torr^{-1} is measured for excitation wavelengths between 400 nm and 500 nm. As the observation frequency is shifted further to the red, the decay rate decreases. For example, a quenching rate $k = 1.3 \times 10^6$ s^{-1} Torr^{-1} is observed for 540 nm emission while exciting at 421 nm.

The decay of fluorescence observed at frequencies near ω_0 represents the collisional relaxation of the sharp vibronic distribution prepared by the optical pulse into lower vibronic levels. The longer decay times observed at red-shifted frequencies are due to the larger number of successive vibrational decays required to deactivate the molecules. Fluorescence is observed as long as the collisionally relaxed NO_2 molecule remains in the energy region between $\hbar\omega$ and $\hbar\omega_0$. The decay rates reported in this work are similar to those reported and explained by Donnelly et al. [6].

The decay rates exhibited by the blue-shifted CO_2 induced fluorescence signals also scale with pressure. The measured decay rates vary between 0.6 k_0 and k_0, with the latter value obtained at low CO_2 laser fluences. The increase of lifetime with fluence is related to increased population in levels which require successive collisional events for complete deactivation. The amplitude versus delay relaxation measurements exhibit the same features. While the fluorescence decay monitors emission from multiphoton excited molecules with energy $> \hbar\omega$ the amplitude decay monitors the population of NO_2 molecules still capable of being excited by a multiphoton process to an energy $> \hbar\omega$. Typical values for k_0' of 0.65 k_0 and 0.95 k_0 were obtained for the amplitude decay when the observation frequency corresponded to blue-shifts of one and two CO_2 photons, respectively.

A comparison of the shape of the prompt (< 30 ns delay) collisionless infrared induced spectrum with the ordinary fluorescence spectrum permits us to extract the absolute probability $P(n)$ for an n-photon absorption event. The distribution function $P(n)$ may also be regarded as an energy distribution function and written as $P(E_n) = P(\hbar\omega_0 + n\hbar\omega_1)$, where $P(E_n)$ is the probability of occupation of that group of levels with energy near $E_n = \hbar\omega_0 + n\hbar\omega_1$ and $\hbar\omega_1$ is the photon energy of the infrared laser. In what follows, we make the *important* assumption that the prompt fluorescence spectrum depends only upon the populations $P(E_n)$ and not upon the method of producing those populations. Then,

$$F(\omega) = \sum_{n=-\infty}^{\infty} A(\omega, E_n) P(E_n), \tag{1}$$

where $F(\omega)$ is the prompt fluorescence signal observed at frequency ω, and $A(\omega, E_n)$ is the fluorescence spectrum produced by a population in that group of energy levels near E_n. In general, $n = 0, \pm 1, \pm 2, \ldots$ corresponding both to emission and absorption of infrared photons. In practice, only a finite group of levels have non-zero population and only a finite number of fluorescence observation frequencies ω_m were monitored. Then eq. (1) can be rewritten:

$$F(\omega_m) = \sum_n A(\omega_m, E_n) P(E_n),$$

which is in the form of a vector equation with matrix elements $A_{mn} \equiv A(\omega_m, E_n)$. The matrix of coefficients A_{mn} can be measured one column at a time by performing the following auxiliary experiment using only visible light: A dye laser is tuned to photon energy E_n and its absorbed energy is measured. This determines a population $P(E_n)$. This population along with the vector of fluorescence signals observed under this condition determines a column of the matrix A_{mn}. Repeating this procedure for different E_n determines the full matrix. With a knowledge of the elements A_{mn}, the matrix can be inverted to give

$$P(E_n) = \sum_m (A_{mn})^{-1} F(\omega_m). \tag{2}$$

If the fluorescence spectrum is known in sufficient detail the populations producing it can be calculated from (2). As a matter of choice, the observation frequencies were selected from the formula:

$$\omega_m \approx \omega_0 + m\omega_1 - 500\ \mathrm{cm}^{-1}.$$

Fig. 4 shows the population distribution resulting from the multiphoton infrared excitation of NO_2 molecules optically prepared by 502 nm dye laser pulses. The CO_2 laser depletes the zeroth level and produces a falling distribution on the high energy side. Due to the small changes in the ordinary Stokes-

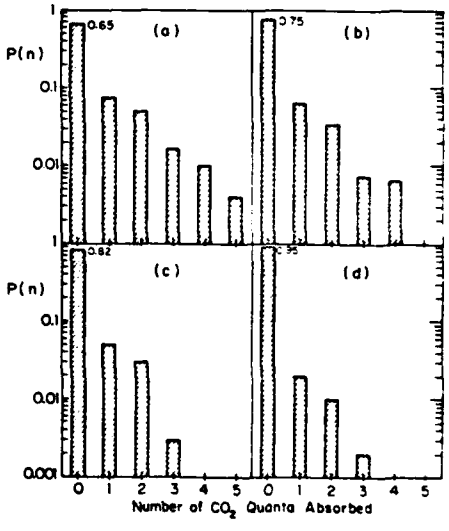

Fig. 4. Histograms of probability $P(n)$ for the net absorption of n photons. (a) 0.5 J/cm^2, (b) 0.3 J/cm^2, (c) 0.2 J/cm^2, (d) 0.1 J/cm^2.

shifted fluorescence signals, the populations at energies less than $\hbar\omega_0$ could not be determined. Presumably a rather symmetrical distribution falling off at lower energies is established.

This procedure for determining $P(n)$ is subject to the very strong assumption that the fluorescence spectrum from levels near E_n is the same whether produced by single photon or multiphoton excitation. Obviously, the selection rules and the precise levels populated may be quite different for the two processes. Nevertheless, the fluorescence spectrum is hardly affected by this difference due to averaging caused by the 1 Å bandwidth of the dye laser and the 50 Å bandwidth of the fluorescence filters. If the differences in fluorescence spectra were important in our case, then we would have seen a fast collisional scrambling signal similar to what was observed by Donnelly et al. [6], but contrary to our observations.

A qualitative survey of the wavelength dependence of the CO_2 laser interaction with optically prepared NO_2 molecules has also been carried out. Blue-shifted fluorescence was observed when tuning over the 9.6 μm and 10.6 μm CO_2 laser lines or tuning the dye laser between 450 nm and 500 nm. This insensitivity to wavelength is surprising in view of the low density of vibrational states of the triatomic NO_2. It implies that exact resonances are probably unnecessary for multiphoton excitation. Indeed infrared multiphoton dissociation has recently been reported in the triatomics OCS [7] and SO_2 [8].

In spite of the rather moderate density of states, a stochastic rate equation approach [9] may describe the temporal evolution of the population $P(n)$. If so, the evolution can be regarded as a random walk along the energy axis with steps of one photon each.

We wish to thank Professor F. Kaufman for making available a preprint of his work and Jerry G. Black for assisting with the computer calculations.

References

[1] E.R. Grant, P.A. Schultz, Aa.S. Sudbo, Y.R. Shen and Y.T. Lee, Phys. Rev. Letters 40 (1978) 115.
[2] V.S. Letokhov and E.A. Ryabov, in: Laser-induced processes in molecules, eds. K.L. Kompa and S.O. Smith (Springer, Berlin, 1979).
[3] J.C. Stephenson, D.S. King, M.F. Goodman and J. Stone, J. Chem. Phys. 70 (1979) 4496.
[4] I. Burak, T.J. Quelly and J.I. Steinfeld, J. Chem. Phys. 70 (1979) 334.
[5] I.P. Herman, A. Javan and R.W. Field, J. Chem. Phys. 68 (1978) 2398.
[6] V.M. Donnelly, D.G. Keil and F. Kaufman, J. Chem. Phys., to be published.
[7] D. Proch and H. Schröder, Chem. Phys. Letters 61 (1979) 426.
[8] S.E. Bialkowski and W.A. Guillory, Chem. Phys. Letters 60 (1979) 429.
[9] J.G. Black, E. Yablonovitch, N. Bloembergen and S. Mukamel, Phys. Rev. Letters 38 (1977) 1131.

Observation of direct infrared multiphoton pumping of the triplet manifold of biacetyl

Appendix 3

Jeffrey Y. Tsao, Jerry G. Black, and Eli Yablonovitch

Gordon McKay Laboratory, Harvard University, Cambridge, Massachusetts

Itamar Burak

Gordon McKay Laboratory and Department of Chemistry, Tel Aviv University, Tel Aviv, Israel
(Received 20 February 1980; accepted 14 May 1980)

Direct collisionless multiphoton (MP) excitation of the triplet vibronic manifold of biacetyl is reported. Following a dye laser pulse which prepares some of the biacetyl molecules in the triplet metastable state, the system is irradiated by an intense 20 ns 9.6μ CO_2 pulse. The CO_2 radiation induces fast quenching of the phosphorescence emission from the ^3A_u excited molecules. It also induces an emission signal in the fluorescence spectral region of biacetyl. This signal is related to intersystem electronic relaxation (IER) from excited triplet vibronic levels into isoenergetic singlet ^1A_u vibronic levels. Analysis of the induced luminescence signals provides information on the collisionless MP prompted vibrational distribution. Excitation with 10.6μ CO_2 pulses leads to the simultaneous MP pumping of both the ground and triplet manifolds. The generation of blue emission signals in this experiment bears a close resemblance to recent observations of prompt visible emission due to MP pumping of ground state molecules. General expressions for the emission intensities are derived with a special emphasis on the specific features of MP vibrational distributions. The detectability of MP induced emission signals is discussed.

I. INTRODUCTION

The collisionless, infrared multiphoton excitation of ground state polyatomic molecules has been the subject of many recent investigations. The diagnostics for the multiphoton process have been:

(a) Optoacoustic absorption measurements[1] followed by the determination of the average number of photons absorbed per molecule;

(b) Observation of multiphoton induced chemistry[2];

(c) Observation of infrared induced emission from the excited molecule[3,4] or from excited reaction products.[5]

Infrared multiphoton excitation of the excited electronic states, however, is still a new research area. In this case, changes in the luminescence are expected to be induced by the vibrational excitation, and thus a powerful new diagnostic is added to the investigation of the infrared multiphoton processes. For example, the collisionless multiphoton pumping of electronically excited NO_2 molecules has recently been reported,[6] in which an analysis of the induced changes in the emission spectra provided an estimation for the n-photon absorption probability $F(n)$.

In this work we report the direct infrared excitation of the triplet state of biacetyl. First, a dye laser pulse pumps the ground state into the ^1A_u first excited singlet state (see Fig. 1), from which intramolecular couplings between the vibronic manifolds of the ^1A_u and ^3A_u electronic states and collision-induced vibrational relaxation lead to the trapping of some of the excited molecules in the metastable triplet state.[7] This state is characterized by a green phosphorescence which originates from a weakly allowed radiative transition to the ground state. Its decay is dominated by a radiationless transition to the ^1A_g ground state, and at room temperature is 1.7 ms as measured from the phosphorescence lifetime.[8] (This value should be compared with the radiative lifetime of 12 msec.[7])

Then, irradiation of the optically excited biacetyl sample with an intense infrared CO_2 laser pulse leads to the excitation of the triplet vibrational manifold. This excitation is characterized by a prompt burst of blue fluorescence, and a fast partial quenching of the green phosphorescence emission. These effects, first observed by Burak, Quelly, and Steinfeld[3] (BQS), have been interpreted as follows. Due to the intramolecular scrambling of the ^1A_u and ^3A_u zeroth order Born–Oppenheimer vibrational manifolds, a new vibronic manifold is formed. The vibronic levels of this manifold are described as a mixture of singlet and triplet vibronic states and consequently carry oscillator strength for emission in both the fluorescence and phosphorescence spectral regions. The observed blue fluorescence signal is due to the CO_2 laser induced accessibility of vibronic levels

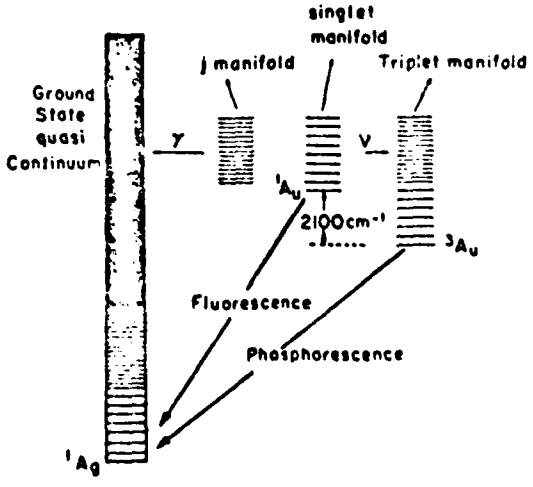

FIG. 1. A schematic diagram of the vibronic manifolds of biacetyl.

with vibrational energy exceeding the singlet–triplet separation energy, and therefore with partly singlet character. The fast drop in the phosphorescence intensity induced by the CO_2 laser is due to the increase, with vibrational energy, in the radiationless transition rate to the ground state. The dependence of this radiationless transition rate $\gamma(E)$ on E has been measured by Van der Werf and Kommandeur.[7]

The previous experiments by BQS[9] involved mainly the indirect vibrational excitation of the triplet manifold. They used 10.6 μ CO_2 laser radiation which preferentially excited the ground rather than the triplet electronic state. The hot ^1A_g molecules then acted as a heat bath for the thermalization of these molecules in the triplet state, thereby increasing the observed phosphorescence decay rate. The present work, using both 9.6 μ, which preferentially excites the triplet over the ground electronic state, and 10.6 μ CO_2 laser radiation, presents evidence for the direct multiphoton pumping of the triplet state. In order to detect an initial nonthermal vibrational distribution, the BQS experiment has been modified. Better time resolution was achieved by shortening the width of the CO_2 laser pulse from 100 to 30 nsec. The use of a more intense, pulsed dye laser instead of a cw argon ion laser provided detectable visible signals from low pressure biacetyl samples. Thus, the lowest pressure in the present experiment was 50 mTorr, while in the former experiment it was 5 Torr. A detailed description of the experimental system is contained in Sec. III. A summary of the theoretical background involving the structure of the mixed singlet–triplet vibrational manifold is presented in Sec. II. The experimental results are summarized and discussed in Secs. IV and V, respectively. In the last section our results will be generalized to the case of light emission due to multiphoton pumping to vibrational levels isoenergetic with the vibronic manifold of an optically active excited electronic state. This case includes the recently observed CO_2 induced emission from CrO_2Cl_2[3] and F_2CO.[4] The theoretical aspects of these inverse electronic relaxation (IER) phenomena have been discussed by Jortner and Nitzan.[10,11] In Sec. VI the IER theory will be used to provide some criteria for the experimental detectability of IER induced emission.

II. THEORETICAL AND EXPERIMENTAL BACKGROUND

The photophysics of biacetyl has been discussed in detail elsewhere.[7,12] The intramolecular interactions between the zero order Born–Oppenheimer singlet and triplet vibronic levels lead to the formation of a single manifold; the $|j\rangle$ levels of this manifold are mixtures of the zero order singlet and triplet states. It is convenient to divide the $|j\rangle$ manifold into vibrational energy regions A and B. Region A is characterized by a low density of zero order singlet vibronic levels. It includes the pure unmixed triplet vibronic states with vibrational energy below E_{ST}, the singlet triplet separation energy. Above E_{ST} each singlet vibronic level $|Si\rangle$ interacts with a set of triplet vibronic levels confined to a width Δ_{ST} around E_{Si}, where

$$\Delta_{ST} = 2\pi v^2 \rho_T \,. \tag{1}$$

v is the mean singlet triplet interaction energy and ρ_T the mean triplet vibronic density. Diagonalization of the molecular Hamiltonian of this set leads to the formation of new wave functions which are admixtures of the $|Si\rangle$ state with the interacting set of triplet vibronic levels. Consequently the A region is divided into "black hole" and "contaminated" subregions. The contaminated subregions consist of mixed vibronic levels, and are confined to strips of width Δ_{ST} around the vibrational energy E_{Si} of the singlet states $|Si\rangle$. The black hole subregions consist of pure triplet vibronic levels, and lie between the contaminated subregions. Region B is characterized by overlapping singlet vibronic levels. More precisely, region B starts at vibrational energies where the homogeneous widths of the singlet vibronic levels $|Si\rangle$ exceed ρ_S^{-1}, the mean separation between adjacent singlet levels. All states in region B are therefore contaminated with one or more zero order singlet states.

Each level $|j\rangle$ in the diagonalized manifold has a width $\gamma_j(E)$ which is the sum of a radiative width γ_j^{rad}, and a nonradiative width γ_j^{nr}, due to irreversible decay into the dense ground state vibronic manifold. Since the nonradiative width dominates over the whole $|j\rangle$ manifold, $\gamma_j(E) \sim \gamma_j^{nr}(E)$. Relations between γ_j and the zero order singlet and triplet level widths γ_S and γ_T have been derived for the two regions.[12] In region A:

$$\gamma_j^A(E) = \gamma_T(E) + \frac{\sum_S \theta(E - E_S)\gamma_S(E_S)}{N_A(E)} \,. \tag{2}$$

The singlet character of the level E_S is diluted by the mean number N_A of interacting triplet vibronic levels, where

$$N_A(E) = \Delta_{ST}\rho_T(E) \,. \tag{2a}$$

$\theta(E - E_S)$ is a step function defined as

$$\theta(E - E_S) = \begin{cases} 1 & -\tfrac{1}{2}\Delta_{ST} < E_S < \tfrac{1}{2}\Delta_{ST} \\ 0 & \text{elsewhere} \end{cases} \,. \tag{2b}$$

In region B:

$$\gamma_j^B(E) = \gamma_T(E) + \frac{\gamma_S(E)}{N_B(E)} \,, \tag{3}$$

where $N_B(E)$ is given by

$$N_B(E) = \frac{\rho_T(E)}{\rho_S(E)} \,. \tag{3a}$$

The emission, due to the presence of zero order singlet-triplet oscillator strengths in the contaminated $|j\rangle$ levels, will be in both the fluorescence and phosphorescence spectral regions, and will have of course the same decay rate in both spectral regions.

These decay rates have been measured in experiments carried out by Van der Werf and Kommandeur.[7] In their experiments, a dye laser was used to optically prepare a state characterized by a zero order singlet vibronic wave function $|Si\rangle$. This $|Si\rangle$ state is a superposition of $|j\rangle$ eigenstates

$$|\Psi(0)\rangle = |Si\rangle = \sum C_j |j\rangle \,, \tag{4}$$

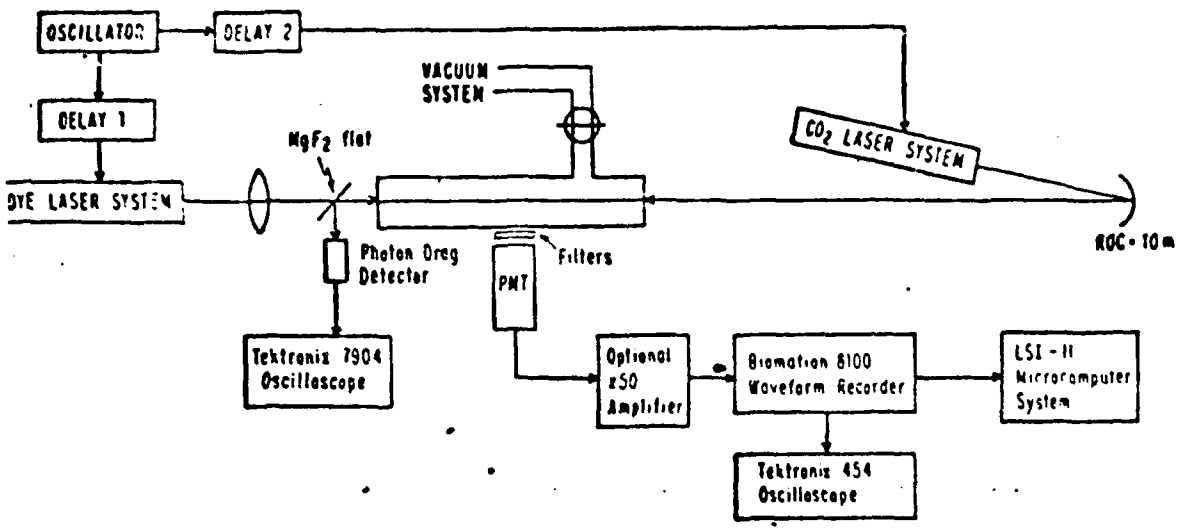

FIG. 2. A schematic diagram of the experimental system.

with a time evolution given by

$$|\Psi(t)\rangle = \sum_j C_j \exp(-iE_j t/\hbar)\exp(-\gamma_j t/2)|j\rangle \ . \qquad (5)$$

The decay of the luminescence emission probability is determined by the quantity $|\langle S|\Psi(t)\rangle|^2$. Lahmani *et al.*[13] have shown that this decay can be expressed as a sum of coherent and incoherent contributions, approximated by a biexponential decay. The fast component is due to the dephasing of the initially prepared superposition, while the long component is a superposition of the independent decays of the excited j levels, and therefore described by the mean decay rates in Eqs. (2) and (3). The dependence of these $\gamma(E)$ on vibrational energy was then determined by measuring the long component of the fluorescence under collisionless conditions, and found to increase steadily with vibrational energy.

II. EXPERIMENTAL

A schematic diagram of the experimental system is shown in Fig. 2. Biacetyl (purchased from Aldrich Chemical Company, 99% purity) was, after freeze–pump–thaw distillations, transferred to a 5 cm diam, 19 cm long Pyrex luminescence cell with NaCl windows at each end. The cell was irradiated in one direction by 30 ns, 20 μJ dye laser pulses whose pump source was a frequency doubled, Q-switched ruby laser. The wavelengths used were in the range of 405–450 nm, and the focused spot diameter was 1 mm. Counterpropagating through the cell in the other direction was a 20 ns, 0.6 J, "truncated" CO_2 laser pulse. The time interval between the two pulses was adjustable up to a jitter of 60 ns *determined by the firing of the CO_2 laser.*

The CO_2 laser pulse was derived from a Tachisto 215 oscillator–plasma shutter–Lumonics TEA 103-1 amplifier system. For a detailed description of the laser system, see Ref. 14. The oscillator output was, via a 4 inch focal length germanium lens, brought to a focus next to an aluminum block onto which a small fraction of the pulse was diverted. The UV radiation caused by the spark on the aluminum block was sufficient to precipitate an avalanche breakdown within the focal region of the main pulse, creating an overdense plasma, and truncating the CO_2 pulse. A 20 ns FWHM pulse with no tail is thereby generated from a 100 ns pulse with a long tail. The shape of the truncated pulse is shown in Fig. 3. The resulting pulse is then amplified, and focused by a 10 m radius of curvature mirror to a 3 mm spot diameter into the luminescence cell. The overlap cross section between the two laser pulses was therefore confined to the central, more uniform part of the CO_2 beam. A MgF_2 flat served the dual purpose of diverting part of the CO_2 beam to a photon drag detector, and preventing damage to the dye laser's glass optics.

The induced luminescence was monitored perpendicular to the excitation beam using either a Hamamatsu R712, or an EMI 9635QB photomultiplier tube, depending on the spectral region, in conjunction with appropriate interference filters. If the signals were weak, they were first passed through an 8 ns FWHM, gain of 50 homebuilt amplifier (consisting of an LM733 video amplifier and an LH033 buffer) before being recorded by a Biomation 8100 Waveform Recorder. The total system response time was, including laser jitter, 80 ns FWHM. After each shot, the data stored in the Biomation was read into a home-assembled Digitial Equipment Corpora-

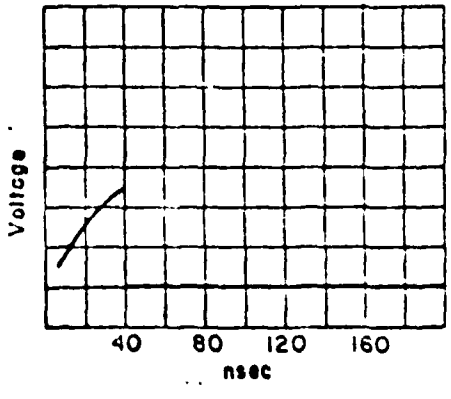

FIG. 3. The truncated CO_2 pulse. Time scale 20 ns/div.

tion LSI-11 microcomputer, and averaged with previous shots.

IV. RESULTS

In this section, the infrared laser induced changes in the characteristic luminescence from the triplet manifold of biacetyl will be described. Biacetyl samples were excited with a pulsed dye laser tuned to 405 nm, and a CO_2 laser fired at a controlled delay following the excitation by the optical pulse. Luminescence was observed in two spectral regions. A narrow band filter centered at 470 nm was used to monitor the blue spectral region; these signals will henceforth be referred to as the fluorescence signals. A long pass filter with a cutoff at 500 nm was used to monitor the phosphorescence; these signals will henceforth be referred to as the phosphorescence signals.

Figure 4 shows the infrared absorption spectrum of biacetyl between 900 and 1200 cm^{-1}. One of the absorption peaks overlaps the CO_2 10.6 μ P branch, but none overlap the 9.6 μ P branch. The CO_2 laser was tuned to the $P(20)$ transitions of both the 9.6 and 10.6 μ bands.

A. 9.6 μ excitation

The effects of the 9.6 μ CO_2 radiation on the phosphorescence signal are exhibited in Fig. 5(a). The optical pulse induces a phosphorescence signal. In the absence of CO_2 radiation, the phosphorescence decays rapidly (on a μs scale) to a quasistationary value, after which it decays slowly with a characteristic lifetime of 1.7 msec. When the phosphorescence intensity attains its quasistationary value, the CO_2 laser is fired. Exposure of the excited system to CO_2 radiation induces a fast decay of the phosphorescence signal from a value I_0 to a value I on a time scale much shorter than the characteristic decay time of the unperturbed phosphorescence. Two main decay components are identified: a fast, pressure independent component with a decay rate greater than 10^7 sec^{-1}, and a slower component, the lifetime of which varies inversely with pressure. Attenuation of the CO_2 pulse results in a smaller drop in the phosphorescence intensity. In order to characterize the drop quantitatively, a yield Y_D is defined as

$$Y_D = 1 - (I/I_0) \,. \tag{6}$$

The drop yield corresponding to a CO_2 fluence of 4.0 J/cm^2 is 0.7. Attenuation of the CO_2 pulse by a factor of two reduces the drop to 0.15, and leads also to the disappearance of the fast component. A lower value is obtained for the drop yield if it is confined to the fast component; a fast drop yield Y'_D is defined through

$$Y'_D = 1 - (I_f/I_0) \,, \tag{7}$$

where I_f is the phosphorescence intensity following the fast decay. Thus a value of 0.4 is obtained for Y'_D at a fluence of 4.0 J/cm^2. The fast drop yield is increased if the delay time between the optical and the CO_2 pulse is decreased. Figure 6 shows the fast drop yield as a function of the delay between the two pulses. As the delay is increased, Y'_D decreases exponentially toward a steady value, at a rate which increases linearly with pressure, and with a value of 3.3×10^6 s^{-1} $Torr^{-1}$.

The induced fluorescence signal [Fig. 5(b)] is characterized by an instantaneous, pressure independent rise

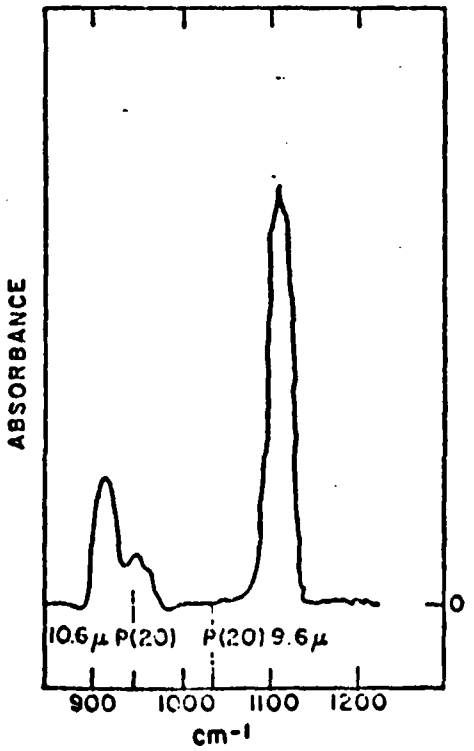

FIG. 4. IR absorbance spectrum of biacetyl.

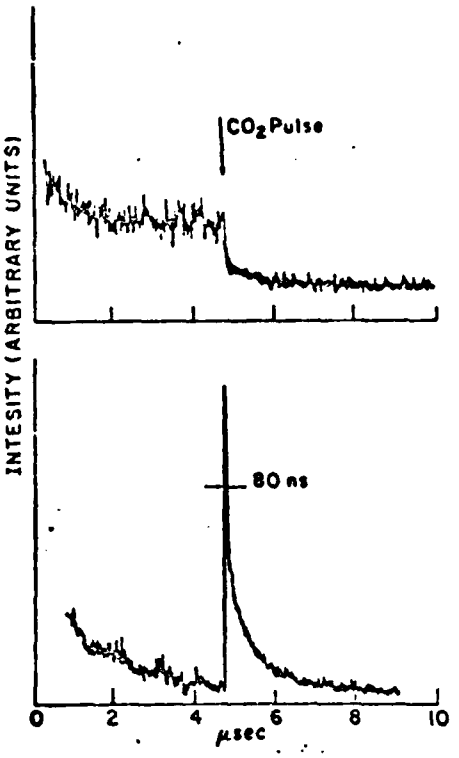

FIG. 5. 9.6 μ induced emission signals. Upper (a) and bottom (b) traces correspond to the phosphorescence and fluorescence emission signals, respectively. The zero time corresponds to the optical excitation by the dye laser pulse. The introduction of the IR pulse is indicated by an arrow.

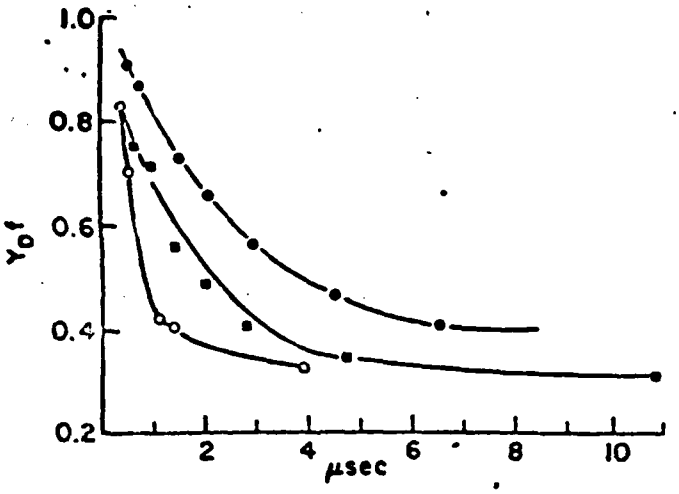

FIG. 6. Y_D^f vs the delay between the visible and IR pulses for various pressures of biacetyl. ● 150 mTorr, ■ 250 mTorr, 500 mTorr.

time, and a decay similar to that observed for the induced phosphorescence signal. The decay times of the long components of the fluorescence and phosphorescence signal exhibit the same $P\tau$ relations. A plot of τ^{-1} vs pressure is shown in Fig. 7; a value of 4×10^6 s^{-1} Torr^{-1} is obtained for the collisional decay rate.

B. 10.6 μ induced signals

Similar to the 9.6 μ case, irradiation with 10.6 μ CO_2 pulses results in a prompt induced fluorescence and a phosphorescence quenching. The rise time of the fluorescence signal is instantaneous and pressure independent. The decays of the 10.6 μ induced signals, however, are characterized by the appearance of a new component whose lifetime depends strongly on the CO_2 laser fluence. Figure 8 shows two typical fluorescence signals, corresponding to high and low fluence. The signals are characterized by an initial spike followed by a longer decay component whose lifetime decreases as the fluence increases. The phosphorescence has the same longer decay component behavior as the fluorescence, but lacks the fast initial decay seen in the 9.6 μ case.

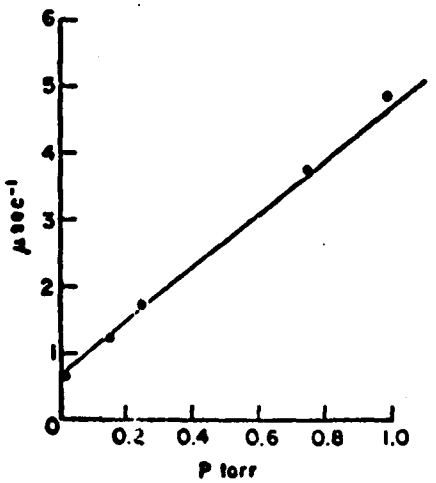

FIG. 7. Quenching rates of the slow component of the 9.6 μ induced fluorescence signal vs the pressure of the biacetyl.

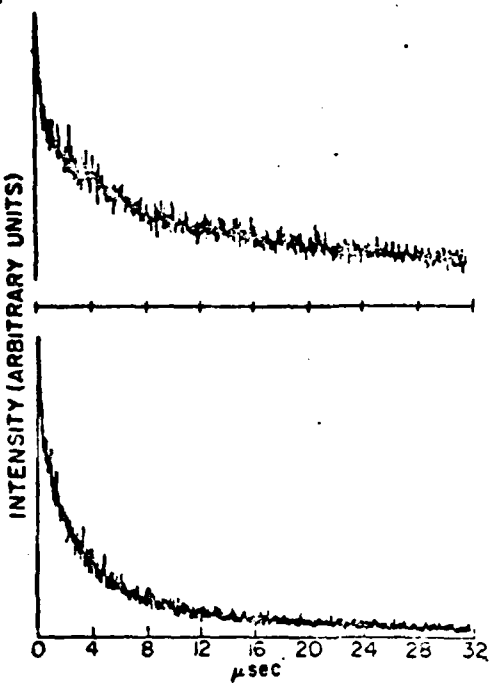

FIG. 8. 10.6 μ induced fluorescence signals from 1 Torr biac biacetyl sample. The upper trace is prompted by 5.0 J/cm² CO_2 pulse. The lower trace is induced by 2.5 J/cm² CO_2 pulse.

V. DISCUSSION

The induced fluorescence and phosphorescence signals reported in the last sections indicate a vibrational excitation within the triplet manifold. The absence of pressure effects on the rise time of the induced fluorescence signals excludes collisional causes; moreover, the short, 30 ns width of the CO_2 pulse ensures a collisionless excitation process. Since the triplet–singlet electronic separation energy is 2100 cm^{-1}, the generation of a blue fluorescence signal sets a lower limit to the accessed vibrational energy of two CO_2 photons.

As a result of the collisionless multiphoton process a nonthermal distribution is established within the triplet manifold. Subsequent changes in the populations of the initially excited vibronic levels are controlled by two mechanisms:

1. An intramolecular conversion into the ground electronic state depletes the population of the excited electronically state. If $n(E)$ is the population density of triplet molecules with vibrational energy E, the depletion rate of this level is given by

$$\frac{d}{dt}n(E) = -\gamma(E)n(E)\ . \tag{8}$$

The intramolecular depletion of the total number of electronically excited molecules N_T is given by

$$\frac{dN_T}{dt} = -\int\gamma(E)n(E)\,dE\ . \tag{9}$$

2. Vibrational relaxation processes due to collisions with ground state molecules lead to vibrational energy redistribution. Ultimately, equilibration between the vibrational temperatures of the ground and triplet electronic states is established.

The fast, pressure independent component of the 9.6 μ induced emission signals is due to the intramolecular decay of molecules excited to high vibrational levels, where radiationless transitions to the ground state are extremely fast. If k is the collisional relaxation rate of molecules excited to vibrational energy E, then the fast component originates from molecules whose vibrational energy exceeds E_f, where E_f is defined by

$$\gamma(E_f) = k \,. \tag{10}$$

The pressure controlled component of the 9.6 μ induced emission signals is due to emission from vibronic levels whose intramolecular decay time is comparable to or longer than the thermalization time τ_{th}. The latter quantity is the characteristic time needed to collisionally relax the vibrational excitation to a room-temperature vibrational distribution. In addition, the dependence of Y'_D on the delay between the dye and CO_2 laser pulses is also due to collisional relaxation. The optical laser pulse prepares a narrow distribution of triplet molecules around the vibrational energy E. When the CO_2 pulse is applied, the optically prepared excited molecules are pumped to vibrational energy regions where the intramolecular decay process dominates. The almost unity value of Y'_D for zero delay times indicates that all the optically prepared molecules have been pumped by the CO_2 pulse to the fast decaying energy region. As the optically prepared vibrational distribution cools, the CO_2 pulse is able to excite fewer molecules to the fast decaying energy region. Finally, the yield reaches a steady value which does not change with further increase of the delay time; this value of Y'_D corresponds to excitation of the thermalized triplet state. Therefore, both the 4.1×10^7 s^{-1} $Torr^{-1}$ collisional quenching rate of the induced fluorescence signal and the 3.3×10^6 s^{-1} $Torr^{-1}$ decay rate of the fast drop yield Y'_D are estimates of the collisional thermalization of the excited vibrational distribution.

Since vibrational excitation is maintained only through the thermalization time τ_{th}, intramolecular radiationless decay is confined to triplet molecules occupying vibronic levels with energy E greater than E_t, where

$$\gamma(E_t) = \tau_{th}^{-1} \,. \tag{11}$$

The determination of Y_D and E_t provides information about the initial vibrational distribution in the following way. Y_D is the fraction of molecules excited to vibrational energies exceeding E_t. 9.6 μ CO_2 pulses with fluence 3.3 J/cm^2 induce phosphorescence signals characterized by a drop yield of 0.65. The thermalization time corresponding to 150 mTorr biacetyl samples is about 1 μs; using the data reported by Van der Werf and Kommandeur, a radiationless decay time of 1 μs corresponds to a vibrational energy of 5400 cm^{-1}. Since Y_D is the fraction of molecules excited to vibrational energies exceeding E_t, 65% of the triplet molecules were excited to vibrational energies exceeding that of 5 CO_2 photons. Another lower limit is obtained by using the fast drop yield $Y'_D = 0.4$. The fast, 100-ns decay time corresponds to an energy of 9 CO_2 photons; thus a fraction 0.4 of the triplet molecules have absorbed more than 9 CO_2 photons. (Since the decay times reported in Ref. 7 were limited to times longer than 300 ns, we extrapolated $\gamma(E)$ using the following approximation[12]:

$$\gamma(E) = A\, e^{BE} + C \,, \tag{12}$$

where $A = 300$ s^{-1}, $B = 1.26\times10^{-3}$ cm, and $C = 82$ s^{-1}.)

Information concerning the 10.6 μ direct MP vibrational excitation is limited due to the appearance of a thermal component. The dependence of the decay time of this component on the fluence of the CO_2 laser has been extensively explored and accounted for by Burak *et al.*[9] The ground electronic state of biacetyl strongly absorbs the 10.6 μ radiation; the average number of photons absorbed per molecule $\langle n\rangle$ determines the rapidly established temperature of the ground state vibrational manifold through

$$\langle n\rangle \cdot h\nu_{CO_2} = \langle E_0\rangle + \left(\int_0^\infty \rho(E) E\, e^{-E/kT}\, dE \Big/ \int_0^\infty \rho(E)\, e^{-E/kT}\right), \tag{13}$$

where E_0 is the mean energy of unexcited biacetyl molecules. Since biacetyl molecules in the ground state constitute the major component in the triplet–ground state mixture, they may be regarded as a heat bath. When a thermal quasiequilibrium between the two vibronic manifolds is established the triplet molecules will decay with a thermalized rate constant $\langle\gamma\rangle$:

$$\langle\gamma\rangle = \left(\int_0^\infty \gamma(E)\rho(E)\, e^{-E/kT} dE \Big/ \int_0^\infty \rho(E)\, e^{-E/kT} dE\right), \tag{14}$$

$$dN_T/dt = -\langle\gamma\rangle N_T \,. \tag{15}$$

An increase in the fluence will result in more photons absorbed, a higher heat bath temperature, and an increased decay rate $\langle\gamma\rangle$.

The instantaneous rise time of the 10.6 μ induced fluorescence signal does indicate some direct infrared excitation of the triplet state, in addition to that of the ground state. The overall transient behavior of the 10.6 μ signals is therefore determined by the following sequence of events. The CO_2 laser excites both the triplet and ground electronic states. While ground state molecules relax to a thermal distribution, the initial nonthermal triplet vibrational distribution relaxes towards the vibrational temperature of the heat bath. When a thermalization is achieved in a time τ_{th}, the residual triplet molecules which have not yet undergone a radiationless transition will decay with the thermalized rate $\langle\gamma\rangle$. The efficiency of the 10.6 μ radiation at directly pumping the triplet state is considerably less than that of the 9.6 μ radiation. The fast, pressure independent decay component of the 9.6 μ induced signals is *not* observed for the 10.6 μ signals, indicating that a negligible fraction of triplet molecules is excited to the vibrational region where the condition $\gamma(E) > k$, is fulfilled. The enhanced efficiency of the 9.6 multiphoton excitation might be related to the red shifting of the ground state IR vibrational spectrum in the triplet state of biacetyl. The relevant ground state spectrum (shown in Fig. 3) consists of the following three bands[13]:

1. A strong absorption band centered at 1115 cm^{-1} assigned to the CH_3 a_u or b_u rocking mode.

2. A 945 cm^{-1}, medium strength absorption band related to the C–CH_3 b_u stretching mode.

3. A 915 cm^{-1} medium strength combination band due to the 539 cm^{-1} and 380 cm^{-1} b_u and a_g bending modes, respectively.

A partial analysis of the vibrational modes of the triplet electronic states has been carried out by Sidman and McClure.[15] The frequencies of some of the analyzed modes are red shifted with respect to the corresponding ground state modes. It is therefore conceivable that the 1045 cm^{-1} $P(20)$ 9.6 μ transaction coincides with the frequency of the strongly absorbing CH_3 rocking mode.

VI. MULTIPHOTON INDUCED IER PROCESS

The generation of induced blue fluorescence emission reported in this manuscript bears a close resemblance to the observation of induced visible emission due to the multiphoton excitation of ground state molecules. Emission induced by high fluence CO_2 pulses has been observed from excited CrO_2Cl_2,[3] and F_2CO[4] samples. Jortner and Nitzan[16] and Burak *et al.*[9] have explained the CrO_2Cl_2 emission as originating from multiphoton excitation to vibrational energy regions where the ground state manifold is scrambled with vibronic levels of an excited electronic state. Jortner and Nitzan have carried out an extensive theoretical study of the inverse electronic relaxation (IER) process leading to the observed emission. Karny *et al.*[3] rejected the IER mechanism in CrO_2Cl_2 on the basis that the ground state density at the origin of the electronic excited state is too high to provide a reversible conversion, suggesting instead the possibility of direct infrared transitions from high vibrational levels of the ground state and low vibronic levels of the excited electronic state.

In this section we shall apply the IER theory to obtain criteria for the experimental detectability of multiphoton induced IER processes. Our treatment will be confined to a $|j\rangle$ vibronic manifold resulting from the scrambling of an excited electronic vibronic manifold $|S\beta\rangle$ with isoenergetic vibronic levels $|G\alpha\rangle$ of the ground electronic state. The width of the $|j\rangle$ levels may be constructed from the zero order widths of the $|G\alpha\rangle$ and $|S\beta\rangle$ states by equations which are similar to Eqs. (2) and (3). Again, the scrambled manifold is divided into regions A and B corresponding to low and high vibrational densities, respectively, of the zero order $|S\beta\rangle$ states. The widths of the $|j\rangle$ levels in region A are given by[10,11]

$$\gamma_j^A(E)=\frac{\gamma_S 6(E-E_{S\beta})}{N_A(E)}, \tag{16a}$$

$$N_A(E)=2\pi v^2\rho_G(E). \tag{16b}$$

In region B the widths are given by

$$\gamma_j^B(E)=\frac{\gamma_S}{N_B(E)} \tag{17}$$

$$N_B(E)=\frac{\rho_G(E)}{\rho_S(E)}. \tag{17a}$$

In contrast to the radiationless decay widths given in Eqs. (2) and (3), the widths γ_j and γ_S in Eqs. (17) and (18) are radiative decay widths. The zero order width γ_S is diluted by the factors N_A or N_B.

Following the collisionless multiphoton process a nonthermal vibrational distribution is established within the $|j\rangle$ manifold. The distribution is characterized by excitation strips of width ΔP_n around the energies E_n, where

$$E_n=nh\nu_{CO_2},$$

$$n=0,1,2,3,\ldots, \tag{18}$$

and ΔP_n is a power broadening width. These excitation strips are populated by the multiphoton process with probabilities $p(n)$.

The rate of photon emission I is the sum of the rates I_A and I_B contributed by molecules excited to regions A and B respectively. To calculate I_A it is convenient to subdivide region A into regions A_I and A_{II}. A_I is the energy region of extremely spare density of $|S\rangle$ levels, viz., $\Delta P_n\rho_S<1$. Region A_{II} is characterized by $\Delta P_n\rho_S>1$. Both regions A_I and A_{II} are of course characterized by $\Delta_{SG}\rho_S<1$. The emission rate from region A_I, I_{A_I}, is given by

$$I_{A_I}=N_0\gamma_S\sum_{n_0}^{n'}\frac{f(n)}{N_A(E)}p(n)\theta'(E_n-E_{S\beta}), \tag{19}$$

where κ_0 is the lowest integer fulfilling $\kappa_0\hbar\omega_{CO_2}>E_{SG}$, $\kappa'\hbar\omega_{CO_2}$ is the boundary between regions A_I and A_{II}, E_{SG} is the separation energy of the G and S origins, and N_0 is the number of molecules in the laser field. $\gamma_S/N_A(E_n)$ is the diluted emission rate from the contaminated $|j\rangle$ levels excited to the nth subregion. $f(n)$ is the fraction of molecules within the nth subregion which are contaminated. $\theta'(E-E_{S\beta})$ is defined through Eq. (2b), except that the homogeneous width Δ_{ST} is replaced by the power broadening width ΔP_n. The introduction of the step function $\theta'(E)$ emphasizes the need for exact resonances in the A_I region: unless there exists an S level within the range Δp_n around E_n, there can be no emissions from the excitation strip around E_n.

In region A_{II} on the other hand, all the excitation strips contribute to the emission. The number of contaminated states within the excited nth region is $\Delta P_n\rho_S$, and therefore

$$I_{A_{II}}=N_0\gamma_S\sum_{n'}^{\kappa_{AB}}\frac{f(n)}{N_A(E)}p(n)\Delta P_n\rho_S, \tag{20}$$

where $\kappa_{AB}\hbar\omega_{CO_2}$ is the boundary between regions A and B, and f_n is estimated as

$$f_n=\Delta_{SG}/\Delta P_n. \tag{21}$$

Substituting (21) for f_n and $\Delta_{SG}\rho_G$ for N_A in Eq. (20) results in

$$I_{A_{II}}=N_0\gamma_S\sum_{n'}^{\kappa_{AB}}\frac{\rho_S}{\rho_G}p(n). \tag{22}$$

In contrast to the MP excitation in region A, each excitation strip in region B contributes to light emission. Since all the $|j\rangle$ levels in this region are contaminated, $f(n)=1$. The rate of photon emission I_B is given by

$$I_B = \gamma_S N_0 \sum_{n \in B}^{\infty} \frac{p(n)}{N_n(E)} = \gamma_S N_0 \sum_{n \in B}^{\infty} \frac{\rho_S}{\rho_G} p(n) \,. \qquad (23)$$

f accidental resonances in region A_1 are neglected, the um rate of photon emission will be given by

$$I = I_{A_{II}} + I_B = \gamma_S N_0 \sum_{n^*}^{\infty} \frac{\rho_S}{\rho_G} p(n) \,. \qquad (24)$$

Since ρ_S/ρ_G is a slowly increasing function of the vi-rational energy E,[12] a lower bound I may be obtained or the photon emission rate from

$$I = \gamma_S N_0 \left(\frac{\rho_S}{\rho_G}\right)_0 \sum_{n=n^*}^{\infty} p(n) \,, \qquad (25)$$

here $[(\rho_S)/\rho_G]_0$ is the density of states ratio at the ori-in of the excited S state. Equation (25) can be used to stimate the plausibility of detecting emission due to a nultiphoton induced IER process. We shall assume that he experiment is limited to detecting photons at a rate aster than 1 photon per μs. Assuming $N_0 = 10^{13}$ and tak-ng the CrO_2Cl_2 molecule values of γ_S^{mc} and $[(\rho_S)/\rho_G]_0$ as $.0^6$ s^{-1} and 10^{-6}, respectively, one obtains that the min-num detectable fraction of molecules excited above $h\nu_{CO_2}$ is 10^{-1}. The CO_2 induced vibrational distribution of CrO_2Cl_2 is unknown, however a value of 10^{-7} for the raction of ground state molecules which have absorbed nore than 20 CO_2 photons does not seem implausible.

Equations (9) and (17) predict long radiative lifetimes for the emitting molecules under collisionless condi-ions. Indeed, 60 μs CO_2 laser induced emission signals nave been detected from 1 mTorr CrO_2Cl_2 samples, much longer than the roughly 1 μs[16] decay times of opti-cally excited CrO_2Cl_2 molecules. If the induced visible emission is observed from high pressure samples, how-ever, a rapid vibrational thermalization follows the ex-citation pulse, and the rate of photon emission is then given by[9]

$$I_{th} = N_0 \gamma_S e^{-E_0/kT} \,, \qquad (26)$$

where T is determined by the average number $\langle n \rangle$ of CO_2 photons absorbed per molecule. A collisional induced quenching has been observed for high pressure (> 1 Torr) of F_2CO and CrO_2Cl_2 samples. In terms of the IER theory quenching may occur only through the disap-pearance of the highly vibrationally excited molecules. The following processes may account for the observed quenching.

(a) An initial nonthermal vibrational distribution is established following the CO_2 laser pulse. The emission intensity characterizing this distribution is determined by Eq. (22). If this intensity is higher than the thermal emission intensity I_{th} determined by Eq. (26), a decay of the initial intensity toward I_{th} will be observed. This decay will be determined by the thermalization time of the system.

(b) A vibrational temperature is established during or following the CO_2 excitation process. The initial emis-sion is determined by Eq. (26), in which T is replaced by a vibrational temperature T_v. Due to the equilibra-tion of the vibrational excitation with the rotational and translational degrees of freedom, T_v is cooled. Conse-quently, the emission decays towards a new value deter-mined by the new temperature T_c common to all degrees of freedom. The difference between T_v and T_c will be significant provided that the vibrational heat capacity is equal to or less than the sum of the rotational and trans-lational heat capacities.

(c) Once the temperature T_c is established, further cooling of the system proceeds only through thermal conductivity or infrared emission, with thermalization times of a few milliseconds. Unimolecular or bimolecu-lar reactive channels could account for observed shorter lifetimes of the emission signals.

An expression for the fluorescence intensity from MP excited vibrational distributions of triplet biacetyl mole-cules is obtained by replacing G by T and N_S by N_T^0 in Eq. (25). Since N_T^0, the number of triplet molecules prepared by the optical pulse is unknown, it is impos-sible to estimate the rate of the induced emission in the fluorescence region. Only a small fraction of the biacetyl molecules is trapped in the triplet state. Typi-cal values of N_T^0 in the present experiment are therefore much smaller than the value 10^{13} assigned previously to N_0 of the chromyl chloride system. Despite the low val-ues of N_T^0, the detection of the fluorescence signals in this experiment is qualitatively explained in terms of the relatively high values of $(\rho_S/\rho_T)_0 \sim 10^{-2}$ and the high value of $\sum_{n=n^*}^{\infty} P(n) \sim 0.5$ achieved by the IR excitation.

ACKNOWLEDGMENT

This work was supported by the office of Naval Research (contract N0014-78-C-0531). One of us (I. B.) is indebted to Professor J. Jortner for helpful discussions.

[1] J. G. Black, E. Yablonovitch, N. Bloembergen, and S. Mukamel, Phys. Rev. Lett. 38, 1131 (1977).
[2] See for example, C. D. Cantrell, S. M. Freund, and J. L. Lyman, in *Laser Handbook*, edited by M. Stich (North Holland, New York, 1973), Vol. 4.
[3] Z. Karny, A. Gupta, R. N. Zare, S. T. Lin, and A. M. Ronn, Chem. Phys. 37, 15 (1979).
[4] J. W. Hudgens, J. L. Durant, D. J. Bogan, and R. A. Coveleskie, J. Chem. Phys. 70, 5906 (1979).
[5] Y. Haas and G. Yahav, Chem. Phys. Lett. 49, 63 (1977).
[6] I. Burak, J. Tsao, Y. Prior, and E. Yablonovitch, Chem. Phys. Lett. 68, 31 (1979).
[7] R. Van der Werf and J. Kommandeur, Chem. Phys. 16, 125 (1976).
[8] F. B. Wampler and R. C. Oldenberg, Int. J. Chem. Kinet. 10, 1225 (1978).
[9] I. Burak, T. J. Quelly, and J. I. Steinfeld, J. Chem. Phys. 70, 334 (1979).
[10] A. Nitzan and J. Jortner, Chem. Phys. Lett. 60, 1 (1979).
[11] A. Nitzan and J. Jortner, J. Chem. Phys. 71, 3521 (1979).
[12] R. Van der Werf, D. Zevenhuijzen and J. Jortner, Chem. Phys. 27, 319 (1978).
[13] E. Lehmann, A. Tramer, and C. Tric, J. Chem. Phys. 60, 4451 (1974).
[14] H. S. Kwok and E. Yablonovitch, Rev. Sci. Instrum. 46, 814 (1975).
[15] J. W. Sidman and D. S. McClure, J. Am. Chem. Soc. 77, 6471 (1955).
[16] J. R. Mcdonald, Chem. Phys. 8, 123 (1975).